remote sensing

MDPI

Article

A Methodological Approach for Assessing the Post-Fire Resilience of *Pinus halepensis* Mill. Plant Communities Using UAV-LiDAR Data Across a Chronosequence

Sergio Larraz-Juan [1,2,*], Fernando Pérez-Cabello [1,2], Raúl Hoffrén Mansoa [1,2], Cristian Iranzo Cubel [1,2] and Raquel Montorio [1,2]

[1] Department of Geography and Land Management, University of Zaragoza, Pedro Cerbuna 12, 50009 Zaragoza, Spain
[2] University Institute of Research in Environmental Sciences (IUCA), University of Zaragoza, 50009 Zaragoza, Spain
* Correspondence: slarrazjuan@unizar.es; Tel.: +34-974482023

Abstract: The assessment of fire effects in Aleppo pine forests is crucial for guiding the recovery of burnt areas. This study presents a methodology using UAV-LiDAR data to quantify malleability and elasticity in four burnt areas (1970, 1995, 2008 and 2015) through the statistical analysis of different metrics related to height structure and diversity (Height mean, 99th percentile and Coefficient of Variation), coverage, relative shape and distribution strata (Canopy Cover, Canopy Relief Ratio and Strata Percent Coverage), and canopy complexity (Profile Area and Profile Area Change). In general terms, malleability decreases over time in forest ecosystems that have been affected by wildfires, whereas elasticity is higher than what has been determined in previous studies. However, a particular specificity has been detected from the 1995 fire, so we can assume that there are other situational factors that may be affecting ecosystem resilience. LiDAR metrics and uni-temporal sampling between burnt sectors and control aids are used to understand community resilience and to identify the different recovery stages in *P. halepensis* forests.

Keywords: forest fire; malleability; elasticity; recovery; vegetation structure; drone; Aleppo pine forests

Citation: Larraz-Juan, S.; Pérez-Cabello, F.; Hoffrén Mansoa, R.; Iranzo Cubel, C.; Montorio, R. A Methodological Approach for Assessing the Post-Fire Resilience of *Pinus halepensis* Mill. Plant Communities Using UAV-LiDAR Data Across a Chronosequence. *Remote Sens.* **2024**, *16*, 4738. https://doi.org/10.3390/rs16244738

Academic Editor: Melanie Vanderhoof

Received: 27 September 2024
Revised: 7 December 2024
Accepted: 11 December 2024
Published: 19 December 2024

1. Introduction

Wildfires are at the core of ecosystems' natural dynamics within the Mediterranean region, being one of the main landscape-shaping agents [1–3], especially when we consider the current context of global change [4–8]. Despite the negative environmental, social and economic impacts it may have, the planet's biodiversity cannot be fully understood without recognizing the role that fires have played as shaping agents in the global distribution of biomes [9,10]. It is expected that both the frequency and intensity of these events will increase [11–16]. This, in turn, will make the analysis of their effects and the evolution and recovery of affected ecosystems key to optimal forest management in terms of ecological sustainability [5,17–19].

In addition to the effects caused by climate change in Mediterranean ecosystems, the anticipated intensification of wildfires is attributable to the abandonment of agricultural lands and the consequent homogenization of the landscape, stemming from the transformation of the social and economic model over the past decades [20–25]. The effects that wildfires have on the physical environment are numerous and are largely dependent on their severity [26–30]. Regarding vegetation, the total or partial combustion of the plant fraction, dehydration and damage, generate greater susceptibility to diseases, fungi and insects. The resistance of plants to fire depends on their physiognomic and physiological characteristics as well as the development of adaptive strategies. Fire affects different parts of the canopy [31–35], with the aerial parts usually being the most damaged [36,37]. In

addition, it also gives rise to effects on the physicochemical and biological properties of the soil and, consequently, hydrogeological processes [38–43]. In summary, these combined effects have consequences on the eco-physiological dynamics themselves, perhaps causing them to become compromised.

In this context, a coevolution of plant communities occurs along with the fires, as they are part of their own evolutionary dynamics [44–47]. In this regard, many typical Mediterranean plant formations, such as *Pinus halepensis*, *Quercus coccifera*, *Quercus ilex* and others, undergo certain transformations that allow for the spatial and temporal continuity of these species, despite—and thanks to—the occurrence of such events [48–51]. Serotiny is an adaptative strategy of *Pinus halepensis* that stores seeds in closed cones to protect them from fire and allows for a massive release of seeds after a fire. Resprouting is the ability to generate new shoots from dormant buds after the aerial fractions have been destroyed by fire [52] and is an efficient fire-resistant mechanism [53], as is the case with *Quercus coccifera*.

Therefore, there is an intense profusion of sprouting and germination mechanisms after the fire, driven by pre-existing species and seeds, which can lead to rapid vegetation cover [45,54]. Regeneration in the case of Aleppo pine forests is well documented [55]. Within a normal fire regime, post-fire regeneration follows a relatively straightforward process [56,57], with high seedling density in the early post-fire stages [58].

Wildfires cause disruption and reformulation in at least three basic dimensions within forest communities: structure, composition and eco-physiological functioning [18,59–61]. In addition to the obvious decrease in coverage and biomass, physiological and morphological changes occur. These modify the factors that influence evolutionary dynamics: water storage capacity, increased runoff, higher surface temperatures, recolonization by better-suited species, etc., [62–64].

The analysis of vegetation structure (e.g., the variability in vegetation height) is one of the key parts of information for its evaluation, due to the role this parameter plays in the functioning and stability of Mediterranean ecosystems [65–67]. The impact of fire on vegetation structure involves the partial or total elimination of biomass, which generates a decrease in structural values, as well as changes to its diversity and complexity that generating a derived ecosystem impact.

In regard to analyzing the effects of fire, the approach concerning the concept of resilience allows us to quantify the levels of recovery attributed to the affected plant communities. Holling defines resilience as the capacity of an ecosystem to absorb changes in state variables, which are produced in response to certain factors that generate damage or stress [68]. He outlines two different ways of envisaging resilience [69]: *Engineering resilience* assumes that there is a state of global stability, and measures resilience as the resistance applied when faced with a disturbance and the speed of return to the equilibrium point; *Ecological resilience* assumes that there can be different alternative stable states, thus referring to the property that mediates the transition between multiple stable states.

Remote sensing is a well-established technique used to monitor active fires [70], as well as their effects in the short, medium and long terms, and, consequently, the recovery process [61,71–75]. Resilience is a property that can be analyzed through the application of remote sensing techniques [71,74,76–80] and by analyzing the structure of the vegetation canopy [81–84].

In recent years, the use of Light Detection and Ranging (LiDAR) has grown exponentially as these sensors allow for the determination of a canopy structure due to their penetrating capabilities [85–88]. LiDAR has the capability to characterize ecosystem structural features relevant to many key elements that determine resilience in forest communities [89–91]. In recent decades, LiDAR sensors, which are mounted on aircrafts, has growing in importance and has been used as a primary resource for conducting forest inventories, determining fuel characteristics, or more directly, related to the effects of fire through analyzing the diversity of forest structure [92–97].

The use of Unmanned Aerial Systems (UASs) to obtain metrics of forest canopy structure in burnt areas is still not widely exploited, despite showing great potential

in the following areas [98–100]: higher spatial resolution than any other platform, low operational costs (ease of acquisition and simple handling), on-demand temporal resolution, avoiding inadequate weather conditions and the capacity to host a wide range of sensors. There are some articles that use UASs to analyze forest structure to develop cartographic products that are related to fuel models [101–103], fire severity [104–106] and fire-induced damage [107–109]. However, as far as we know, there is a gap in the employment of UASs to measure the recovery of forest structures in Mediterranean ecosystems in the medium and long terms.

In this article, using LiDAR data obtained from UASs, we are focus on two particular properties of resilience from the point of view of engineering resilience [110]:

- *Malleability* is a quantifiable property that describes the degree of similarity between two steady states separated by a disturbance, thus enabling the assessment of the degree of recovery for affected plant formations [111].
- *Elasticity* is a property of resilience that describes, through a measurement of time, the speed at which systems return close to their initial state after a disturbance [111,112].

Both properties can be analyzed through LiDAR-UAS data across a chronosequence. With the different fires being examined from a qualitative point of view, the degree of similarity/dissimilarity among the structures of the burnt areas and the control areas will define the degree of malleability (more similar = less malleability). To analyze elasticity, these differences will be quantified in temporal terms, depending on the number post-fire years that have elapsed.

In view of this, this study aims to evaluate post-fire vegetation recovery by comparing burnt and control sectors using LiDAR metrics related to vegetation structure (canopy height, density and physiognomic complexity). The study focuses on Aleppo pines with kermes oak formations (*Ph-Qcc*) that were affected by four forest wildfires that occurred over four different years, approximately during the last 50 years. Said years are 1970, 1995, 2008 and 2015.

For the purpose of analyzing resilience in these typical Mediterranean formations, a diachronic analysis will be conducted from a uni-temporal perspective (i.e., fires that occurred in different years will be analyzed from a specific moment in time). In this regard, areas of analysis have been delimited, which include burnt sectors from different fires and their respective control sectors, connected to burnt sectors, to ensure that the comparative analysis is equitable.

We hypothesize that: (a) the accuracy and precision of UAS data allow for the detection of variations in structure, resulting from different stages of post-fire ecosystem evolution; and (b) the experimental design, which is based on the analysis between burnt and control zones located in different forest fires, enables the quantification of resilience in terms of malleability and elasticity.

2. Materials and Methods

2.1. Study Area

The wildfires affected Aleppo pine (*Pinus halepensis* Mill.) stands with Quermes oak (*Quercus coccifera*) in two different areas—although both share environmental characteristics—located in the province of Zaragoza, in Aragón (Spain). First, in the Montes of Zuera region (Zaragoza, Spain), fires occurred in 1970, 1995 and 2008. Second, in the Sierra de Luna (Zaragoza, Spain) region, the most recent fire took place in 2015. This area was chosen because, over a small portion of land, numerous incidents appear, separated by time, affecting the same plant community and, therefore, having shared environmental characteristics. These fires were representative of the fire regime in the area.

The chosen areas, shown in Figure 1, were representative of each fire and sufficiently accessible. With this goal in mind, preliminary diagnostic work was carried out in the office, which consisted of analyzing orthophotographs and cartography derived from DEM (downloaded from the National Center of Geographic Information). In addition, these areas allowed the UAS device to connect to Real-Time Kinematic (RTK) positioning, called

ARAGEA, which is used to provide highly accurate positioning and navigation data. To verify the representativeness of this, severity levels were extracted from selected footprints using Montorio et al.'s methodology (2020), and it was confirmed that the severity level of the Burnt Plots matched that of the fires [113]. In accordance with Tobler's First Law of Geography [114], both the burnt and control sectors were closely situated, to ensure the environmental homogeneity of their characteristics. With the same objective in mind, the burnt areas were spatially connected to unburnt areas, that can serve as controls (i.e., areas with the same characteristics prior to the disturbance). Although, this choice of control zones can lead to cross interference, ensuring that the environmental and morpho-topographic conditions are as homogeneous as possible and, ultimately, exhibit maximum similarity, meaning that this experimental area design was chosen. The severity smoothing factor that could arise from the choice of a terminal zone for the fire was not determined, as confirmed in the aforementioned severity analysis.

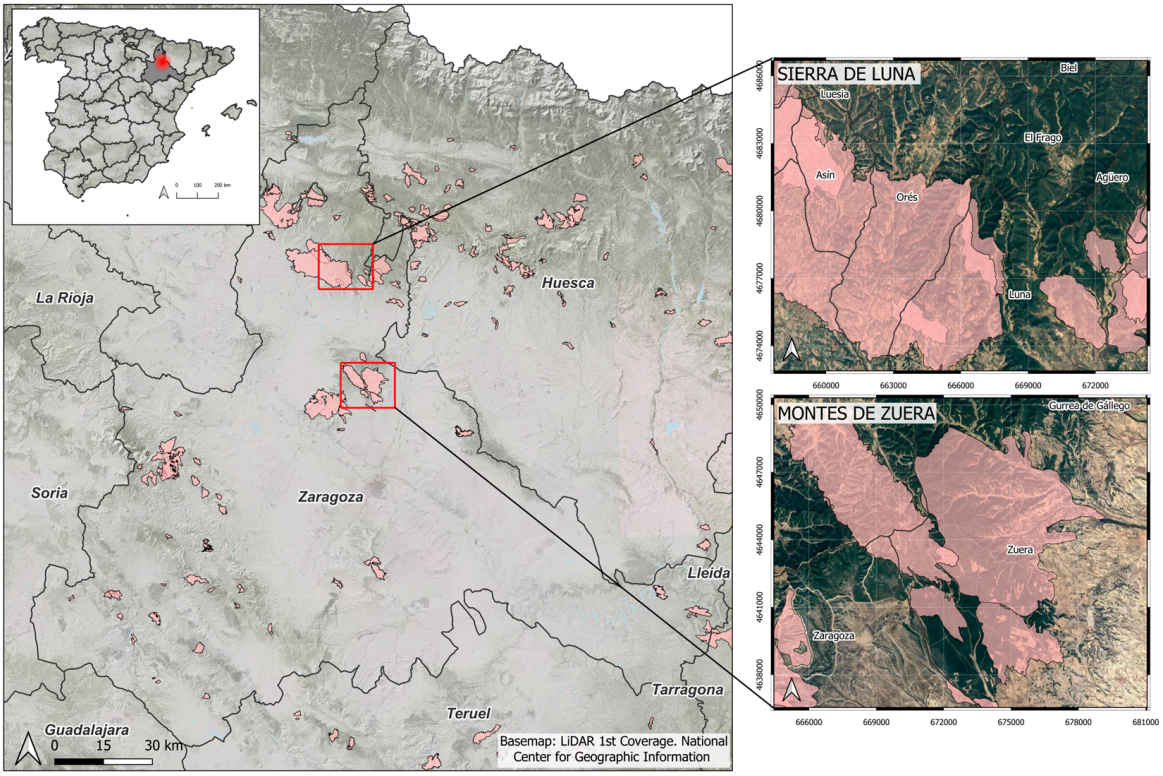

Figure 1. Study area localization (EPSG: 25830). In light pink: contours of burnt areas in Aragón (Spain).

Both areas are approximately located within a spatial range of 25 to 50 km northeast of Zaragoza, Spain. The average elevation ranges from 500 to 750 m above sea level, on top of a structural platform formed by Miocene carbonate, as well as marl and sandstone sediments, arranged on horizontal strata. The terrain is undulating, with a wide variety of valley-slope succession orientations, resulting in a configuration of main and secondary valleys [115].

The area has a Mediterranean continental climate, with an average annual temperature ranging from 11 °C to 13 °C. The average monthly maximum temperatures during the summer reach around 30 °C, often exceeding this mark. Daily maximum temperatures can reach up to 40 °C. The average monthly temperatures during the winter reach around 5 °C, with frequent frosts. Seasonal and daily temperature variations are significant, with a range of more than 15 °C in both cases. The average annual precipitation is over 450 L/m^2, with minimum levels in the summer and frequent droughts [116].

2.2. UAV Data Acquisition

In the first phase of the process, four flights were conducted in the spring of 2023: 16 March for the 1970 fire, 22 March for the 1995 and 2008 fires and 3rd March for the 2015 fire. The Unmanned Aerial Vehicle (UAV) used was the DJI Matrice 300 RTK, a quadcopter equipped with a DJI Zenmuse-L1 LiDAR sensor. This sensor operates at a wavelength of 905 nm, with a range of 450 m and an accuracy of 2–3 cm. This high spatial resolution guarantees that the structural characteristics of the vegetation can be precisely monitored and in detailed scale. The UAV is also equipped with an optical camera and an enhanced inertial measurement system by DJI.

As mentioned previously, plots were defined in fire-affected areas during different years, along with their respective contiguous Control Plots, so that we could observe and quantify differences. The recovery rate of the post-fire plant structure was analyzed from a single moment in time, so as to observe the different regenerative dynamics (thus the degree of malleability) depending on the time elapsed. The uni-temporal nature of the measurements ensured that the comparative analysis was equitable. This approach, using a linear matrix method, implies the absence of corresponding elements (pixels), thereby ensuring that any differences between burnt and control sectors reflect different regeneration patterns.

As can be seen in Figure 2, the flight plan was plotted over areas covering approximately 6–10 hectares, with contiguous passes at a constant altitude of 100 m above the Digital Elevation Model (downloaded from the National Center of Geographic Information-PNOA Project). The average flight speed was 7 m/s, with a transverse and frontal overlap of 80%, resulting in a point density of approximately 450 points per square meter.

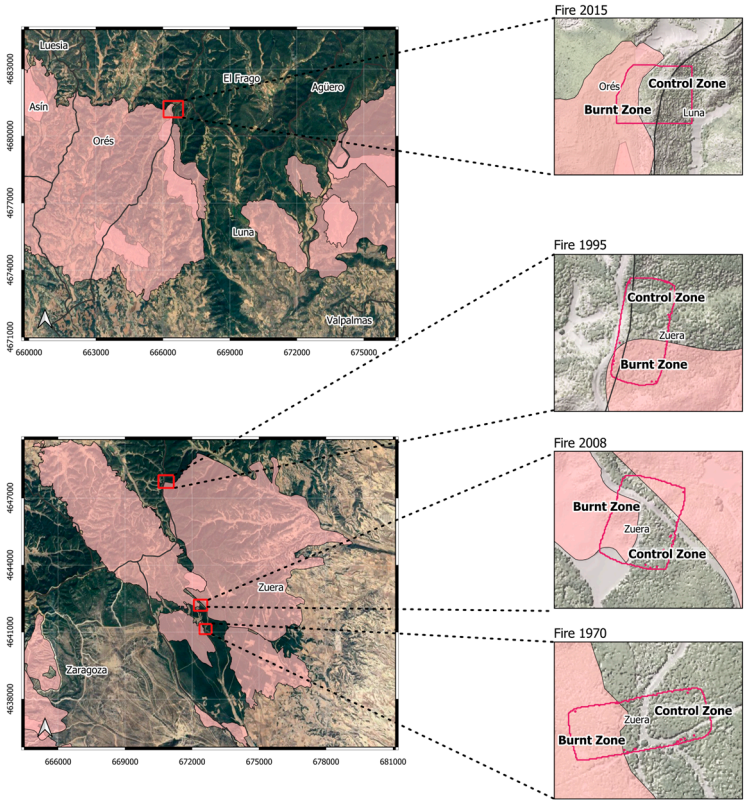

Figure 2. Flight footprints, located in Sierra de Luna (SL) and Montes de Zuera (MZ), corresponding to the fires in 1970, 1995, 2008 (MZ) and 2015 (SL). EPSG: 25830. In light pink: contours of burnt areas. In magenta: drone footprints.

2.3. UAV Data Processing

The data collected were processed using DJI Terra v 4.21 software, designed to reconstruct 3D models, which allowed for data extraction and conversion to the .las format. Data cleaning, ground point classification and height normalization were conducted following Montealegre et al. (2016), using the MCC-LiDAR version 2.1. command line tool [117,118].

Within the flight footprints, smaller homogeneous areas were delimited to capture the structural variability in the burnt sectors and their respective controls (Figure 3). This was performed without overcomplicating data processing due to their large volume. The plots (burnt and control for each fire) were 1600 m^2, ensuring that the topographic parameters (orientation and slope) were comparable, as differences between these parameters can lead to differential structural characteristics. The average distance between burnt and control sectors is 171.75 m. This criterion of contiguity and minimum distance aims to ensure maximum similarity between sectors, as mentioned in the previous section.

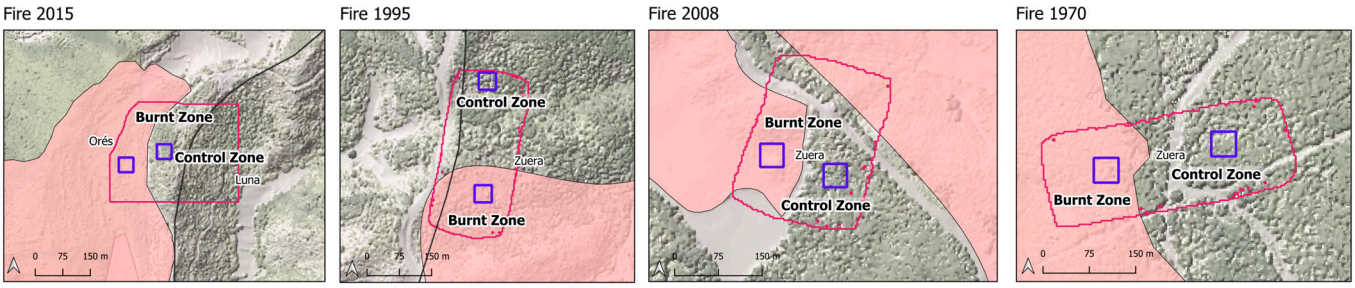

Figure 3. Experimental scheme with quadrangular sectors (analysis plot) corresponding to the burnt and control sectors (EPSG: 25830). In light pink: contours of burnt areas. In magenta: drone footprints. In violet: analysis plots—burnt and control—of each fire.

Forest structural metrics were extracted at the plot scale using FUSION/LDV v.4.21 software. These metrics that have been used in other studies [90,119,120] allowed us to characterize the forest structure accurately, thanks to a spatial resolution of 0.5 m. Canopy Cover is the proportion of the ground covered by the vertical projection of the vegetation and tree (or shrub) crowns. The analysis of Canopy Cover (CC) was conducted using a pixel size of 5 m. This should be larger than the tree coverage area, so as to avoid erroneous estimations [121].

$$CC = \left(1 - \frac{\sum_{i=1}^{n} z_{iz>0.05}}{n}\right) \times 100 \quad (1)$$

where i is the laser return, n is the total number of returns and z is the height of the LiDAR return, taken with a minimum threshold of 5 cm.

Height distribution is represented by the mean height (Hm) and the 99th percentile (P99), while height variability is captured by the coefficient of variation (CV).

$$CV = \frac{\sigma}{\overline{X}} * 100 \quad (2)$$

where σ is the standard deviation and $\overline{X}$ is the mean height of the LiDAR returns for each pixel.

The Canopy Relief Ratio (CRR) is a measure (0–1) that indicates whether the canopy is positioned at the top (>0.5) or bottom (<0.5) of the pixel.

$$CRR = \frac{\overline{Z} - Z_{min}}{Z_{max} - Z_{min}} \quad (3)$$

where Z_{min}, Z_{max} and $\overline{Z}$ are the minimum, maximum and mean height of the LiDAR returns for each pixel.

These indicators of cover (Canopy Cover), mean and percentile of height (height mean, 99th percentile); diversity (coefficient of variation, Canopy Relief Ratio); and complexity (Profile Area Change) are representative of the physiognomic characteristics of forests and, therefore, can be used to infer many ecosystem functions [90]. While the indicators of height (Hm and P99) and the percentage of cover (CC) may affect the gas exchange process for photosynthesis, the amount of light received and, therefore, the productivity and carbon storage [122,123] diversity (CV, CRR) are related to understory competition, species composition and diversity [124,125].

Hu et al. (2019) introduced two multitemporal metrics: Profile Area (PA) and Profile Area Change (PAC) [126]. PA determines the degree of vertical stratification connectivity, because it assesses biomass at different height strata through the vertical distribution of LiDAR returns.

$$PA = \int_0^{100\%} f\,(percentile)\; d\,(percentile) \tag{4}$$

PAC describes changes between burnt and control sectors by carrying out a simple subtraction.

$$PAC = PA_{pre} - PA_{post} \tag{5}$$

Profile Area is a metric that can help us quantify the structural changes produced after fires [126]. In this paper, we use it as a proxy to analyze resilience, given that it is related to structural complexity. Therefore, it connects with ecosystem functions.

Moreover, the percentage of vegetation coverage per unit area (Canopy Cover—CC) was analyzed, along with strata-level analysis, by adapting the Bertrand design (1966) [127]. The calculated metrics are the percentage of each stratum relative to the total pixel and associated coefficient of variation defining the following levels: <0.5 m (lower understory); 0.5 m–1 m (upper understory); 1 m–3 m (shrub layer); 3 m–5 m (undertree layer); and greater than 5 m (tree layer).

Finally, Geographical Information Systems (GISs) were used for spatial data visualization (ArcGIS for Desktop 10.8.1), as well as for the incorporation of additional informational parameters.

2.4. Statistical Analysis

The statistical analysis applied was organized into three levels:

Firstly, different types of comparison analysis were developed (Cumulative frequency distribution—Kolmogorov–Smirnov and Mann–Whitney U tests for independent samples) to determine the differences between selected metrics in burnt vs. control sectors for each year. D-statistic (K-S) was used to demonstrate the magnitude of differences between Burnt Plots (BPs) and Control Plots (CPs), as it is sensitive to differences in both the location and shape of the cumulative distribution function. The statistical probability associated with the U statistics allows us to surmise whether there are differences between the analyzed groups or not. Secondly, the influence of disturbance age and the fire factor (BP/CP) were analyzed using variance analysis, considering the combined effect resulting from the interaction between both factors.

Given the non-parametric nature of the data, a Kruskal–Wallis analysis was performed, which serves as a proxy for the explained variance in *R squared* from the ANOVA analysis. Following Sheskin, 2003 [128], the proportion of variation in the ranges explained by the different groups is expressed through the *η squared* statistic. Thirdly, statistical parameters of dispersion—coefficient of variation—were used for strata coverage data, relative to the total pixel surface area (including those corresponding to ground surface).

3. Results

3.1. Coverage Analysis

In Figure 4, a greater diversity in percentage coverage, across all areas, is observed in the control sectors (CPs) compared to the burnt sectors (BPs) (i.e., the interquartile range is wider in CPs compared to BPs), given the 5 m pixel size.

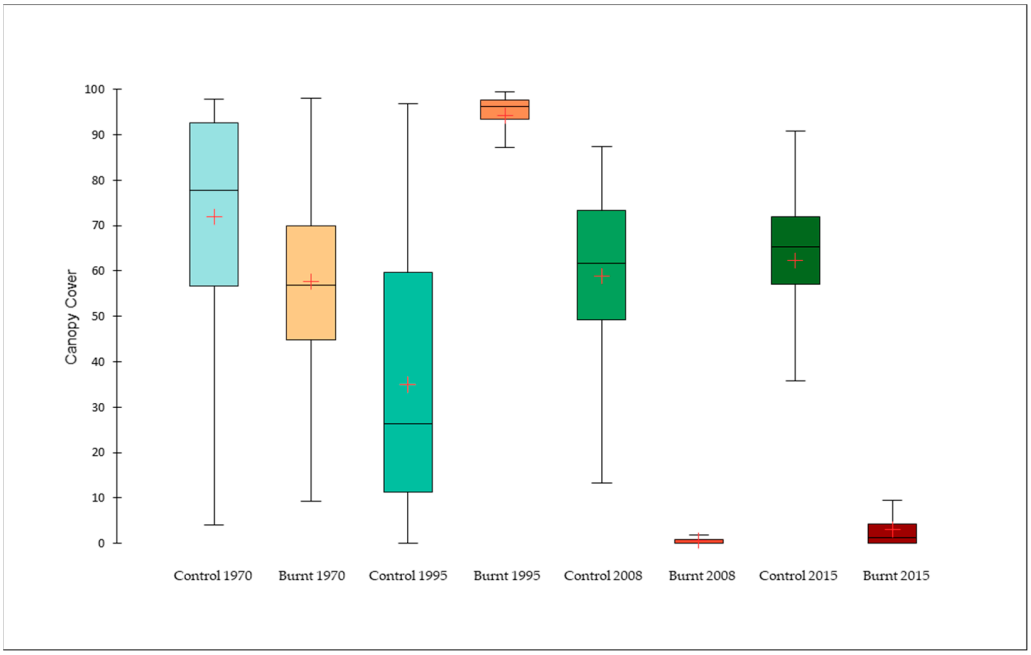

Figure 4. Boxplot of Canopy Cover (percentage of ground covered by the vertical projection of the vegetation) in different sectors (BP/CP) by year of fire. In green: Control Sectors; in red: Burnt Sectors. Boxes are arranged chronologically (most recent on the left and oldest on the right). The orange cross represents the mean value.

The Interquartile Range (IQR) of the control sectors is consistently higher, resulting in a higher percentage of Canopy Cover in CPs compared to BPs, except in 1995 where the entire IQR of BPs is above 90%. This CP > BP difference increases with each passing fire (except in 1995), although the BP values in 2008 are lower than those in 2015.

In general, a very homogeneous response is observed between sectors from the 1970 fire, in contrast with what is observed in the more recent fires, where most cases are concentrated below 10%. Meanwhile, the 1995 fire shows exceptional characteristics, with all cases concentrated above 90% in BPs.

In Appendix A, coverage percentage charts by strata are included to analyze stand density across different canopy levels (Figures A1–A4).

Table 1 shows the evolution of differences between sectors. Significant differences ($p < 0.05$) are observed between sectors in all cases, with the actual magnitude and the D indicator increasing as the fire's age decreases. The exception is 1995, which shows the highest difference in value, but with a contrasting trend compared to the others (BP > CP, whereas in the rest CP > BP).

Table 1. Differences of Canopy Cover between sectors (Burnt Plot–Control Plot) by wildfire, and magnitude of these differences, shown with D-statistic.

Year	Difference (%)	D Statistic
1970	−14.248	0.406
1995	59.193	0.906
2008	−58.147	0.984
2015	−59.293	0.969

3.2. LiDAR Metrics

The characterization of the structure was conducted using the metrics described in Section 2.1. The cumulative relative frequency plots for each metric illustrate the degree of similarity–dissimilarity among the regenerated structures and their respective controls

(Figure 5). The statistical significance of the information collected in this Figure is outlined more specifically in Table 2.

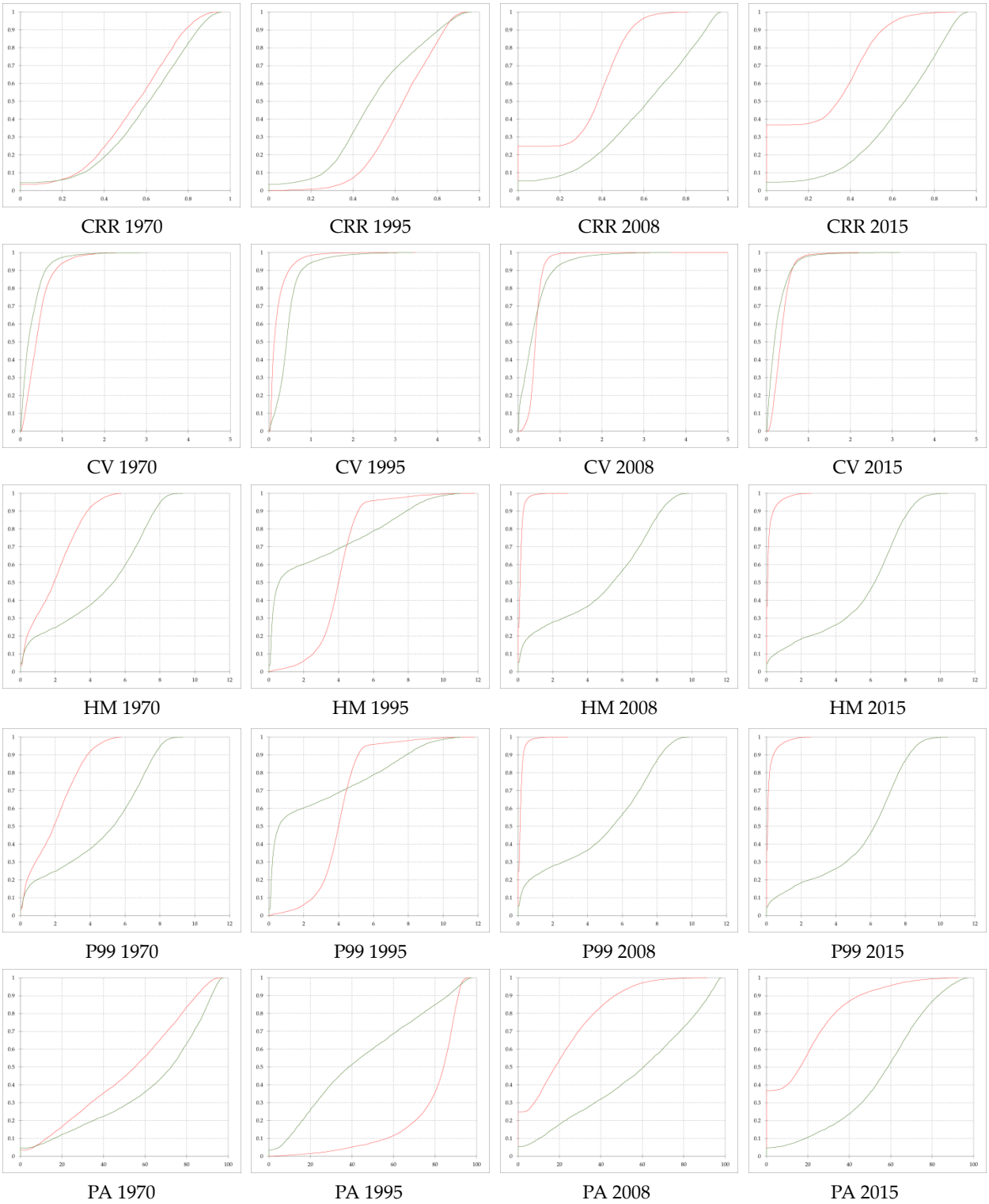

Figure 5. Distribution of cumulative relative frequencies (in green: Control Sectors; in red: Burnt Sectors) by wildfire for Canopy Relief Ratio (**first row**), coefficient of variation (**second row**), height mean (**third row**), 99th percentile (**fourth row**) and Profile Area (**fifth row**). Graphics are arranged chronologically (most recent on the left and oldest on the right).

The **Canopy Relief Ratio (CRR)** shows an association in distribution for the oldest fire (1970). However, in the other three fires, there is a clear asymmetrical factor that increases in the more recent fires. The "step" located around zero in the different plots defines the number of ground pixels for each sector. In 1995, there is a higher concentration of canopy at the top of the burnt area, whereas in the more recent fires (2008 and 2015)—which exhibit similar distribution characteristics—there are abundant ground pixels, notably higher in the 2015 fire.

The **height mean (Hm)** displays a clear pattern of similarity in the more recent fires, where the largest differences are recorded: CPs have a normal distribution, and there is a concentration of almost all cases of BPs below 2 m. In the case of 1970, there is a breakpoint starting from 0.3 m, highlighting the lower height in BPs, which records all cases below six meters. The 1995 control shows a distribution with a certain concentration of pixels with low height (<1 m), while the canopy of colonizing communities shows dominant heights between 2 and 5 m.

In the **coefficient of variation (CV)** analysis, the ground pixels have not been included to avoid potential distortion factors and to enhance comparability across different fires. Therefore, this action will be conducted later. There is a certain similarity in the shape of the histograms: curves clearly associated between burnt and control areas for the years 1970 and 2015. The CV is lower in CPs, indicating greater homogeneity in canopy height variability. The 1995 fire presents a contrasting situation, where the BP is more homogeneous than the CP. In the 2008 fire, the pattern is comparable to 2015, albeit with an intersection around 0.3.

The **99th percentile (P99)** shows distribution features almost comparable to its mean height, but with a slight shift on the coordinate axis for all cases. The largest differences are found in the year 2008, where no values above 2 m are observed for BPs, while in CPs, 80% of the pixels are above 4 m and even reach heights exceeding 10 m. The year 2015 exhibits a similar pattern, although CPs show a slightly greater concentration in the higher values.

The **Profile Area (PA)** is a measure of canopy structural complexity Akin to the CRR. There is a "step" observed at the 0 value, which defines the number of ground pixels. Different distributions are observed between sectors, except for the 1970 fire, which presents an association. The BP profiles of the more recent fires exhibit a logarithmic character and are positioned above CPs. In the case of 1995, the profiles show a highly asymmetrical character, running below CPs. The application of **Profile Area Change (PAC)** yields positive values for the fires in 1970 (11.66), 2008 (34.70) and 2015 (36.21), and negative for 1995 (−34.67). Therefore, for 1995, there is higher complexity and density of regenerated vegetation compared to other years, while 1970 shows greater similarity between regenerated structures and their controls.

In Table 2, the **differences in metrics—both absolute and normalized** for comparability—between burnt sectors and their respective controls are outlined.

Table 2. Absolute differences (Burnt Plot–Control Plot) and normalized differences (BP − CP/BP + CP) of the various metrics analyzed for year. Acronyms: CRR = Canopy Relief Ratio; CV = coefficient of variation; Hm = height mean; P99 = 99th percentile; PA = Profile Area. Significant differences between burnt sectors and their controls are analyzed with the D-statistic (Kolmogorov–Smirnov test).

	Year 1970		**Year 1995**		**Year 2008**		**Year 2015**	
Metrics	**Dif (abs)**	**Dif (nor)**	**Dif (abs)**	**Dif (nor)**	**Dif (abs)**	**Dif (nor)**	**Dif (abs)**	**Dif (nor)**
CRR	−0.047 *	−0.042 *	0.129 *	0.114 *	−0.268 *	−0.295 *	−0.339 *	−0.380 *
CV	0.159 *	0.222 *	−0.261	−0.382	0.022	0.027	0.098	0.154 *
Hm	−2.588 *	−0.400 *	1.334 *	0.202 *	−4.529 *	−0.937 *	−5.202 *	−0.944 *
P99	−2.661 *	−0.326 *	1.242 *	0.147 *	−5.586 *	−0.909 *	−6.155 *	−0.922 *
PA	−11.663 *	−0.102 *	34.668 *	0.285 *	−34.704 *	−0.457 *	−36.213 *	−0.495 *

* Differences are statistically significant, with a threshold of 0.01.

Generally, increasing differences are observed as the fire age decreases, except for CV, Hm and P99 in the year 1995. This fire exhibits a different recovery behavior compared to the metrics of all the others, indicating its anomalous nature (i.e., the regenerated structures show greater development, complexity, higher relative form and structural homogeneity in the burnt sector, in contrast to the other fires). In Appendix A, the differences between the burnt sectors of the different fires are shown (Table A1).

The ground pixels (Table 3) show a similar number of cases in the control areas for different fires. However, in the burnt areas, there is a clear increase in the more recent fires, resulting in a larger area with no vegetative growth (less than 5 cm).

Table 3. Ground pixels (Burnt Plot–Control Plot) in the analyzed fires and the difference between both. Over a total of 6400 pixels for each type of plot.

Year	Burnt	Control	Dif (Burnt–Control)
1970	229	292	−63
1995	10	233	−223
2008	1592	341	1251
2015	2357	308	2049

In Figure 6, we can observe that the magnitude of the differences—indicated by the lines of the D-statistic—increases with each passing fire, except for the CV, which shows the opposite trend. However, as we have corroborated, the 1995 fire disrupts the pattern of the analyzed regeneration process, as the differences in trends change compared to the other fires.

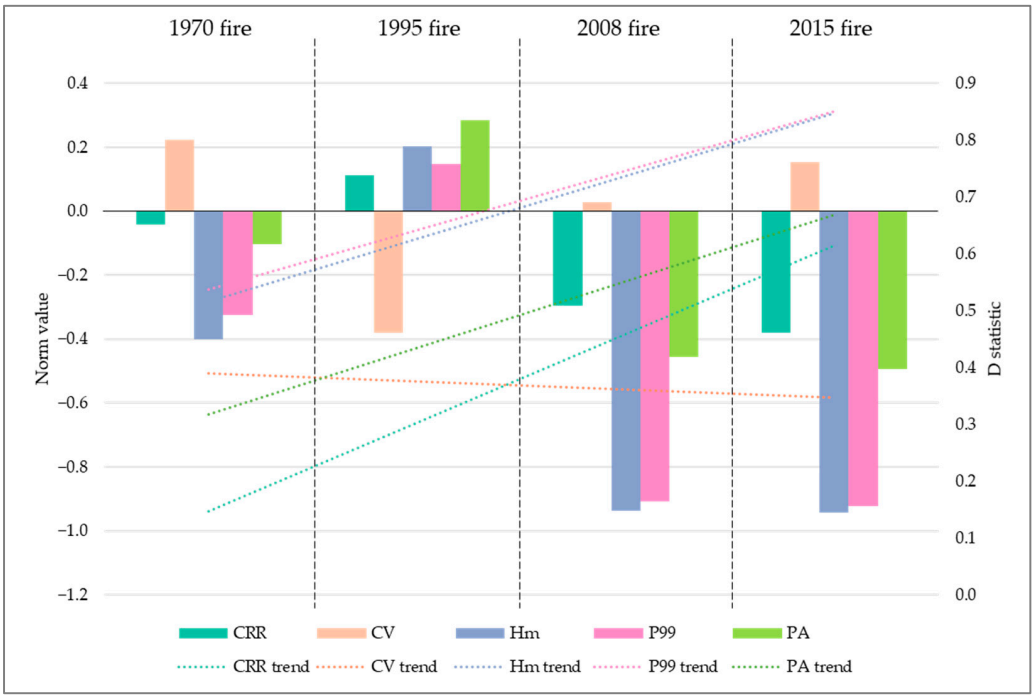

Figure 6. In lines: trend of magnitude of differences, expressed through the Kolmogorov–Smirnov statistic D. In bars: normalized differences of the analyzed metrics: mean height, 99th percentile, coefficient of variation, Canopy Relief Ratio and Profile Area.

The **Kruskal–Wallis** analysis (fire age and type of sector —burnt/control— vs. both factors) shows the complementarity of the factors analyzed, since the interaction between both improves the explanatory capacity of the models, at least doubling it for all metrics, especially in the CV (Table 4). The explained variance ranges from 15.9% for the CV to 49 for P99 and height mean.

Table 4. Results of adapted Kruskal–Wallis analysis (η^2). Central column [$\eta^2_{(\text{without interaction})}$] shows the result of the analysis without an interaction between fire age and type of sector. Right column [$\eta^2_{(\text{with interaction})}$] shows the result of the analysis with an interaction between both variables. Acronyms: CRR = Canopy Relief Ratio; CV = coefficient of variation; Hm = height mean; P99 = 99th percentile; PA = Profile Area.

Metric	$\eta^2_{\text{(Without Interaction)}}$	$\eta^2_{\text{(with Interaction)}}$
CRR	0.109	0.254
CV	0.025	0.159
Hm	0.265	0.495
P99	0.289	0.498
PA	0.163	0.375

3.3. Characterization by Strata

The **percentage of coverage by strata**, according to the height ranges outlined (<0.5 m; 0.5 m–1 m; 1 m–3 m; 3 m–5 m; >5 m), allows the vertical profile of vegetation structure to be characterized. In Figure 7, strata distributions are shown, with regard to the time period that has elapsed between fires and drawing a space between graphs in proportion to this.

In the more recent fires (2015 and 2008), the sum of the percentages of the lower strata (<0.5 m and 0.5 m–1 m) constitutes nearly 100% of the burnt areas. A more advanced state of recovery can be observed after the 2008 fire, since the percentage of ground cover is lower in this one (24.88% for 2008 vs. 36.83% for 2015) and the percentages of the 0.5 m to 1 m level are higher: 71.64% and 57.11%, respectively. The intermediate strata (1 m to 5 m) show minimal coverage (0.78% for 2008 and 2.66% for 2015) compared to their controls, while the upper strata have no representation (<0.01%), with the highest level (upper than 5 m) predominating in their respective CPs.

In the 1970 wildfire, the upper stratum (>5 m) is not as extensively represented in BPs as in CPs (2.70% vs. 48.90%). Conversely, the following levels (1 m to 5 m) have a much higher coverage in BPs (52.03%) than in CPs (18.78%). Similarly, the lower stratum (0.5 m to 1 m) shows notably higher coverage in BPs than in CPs (more than 10% difference).

In the case of the 1995 fire, a different pattern is observed compared to the other wildfires. The undertree level (3 m to 5 m) covers 65.52% of BPs, while in its control area it only covers 5.82%, indicating a similar trend of massive and homogeneous growth of regenerated structures. However, the first level (lower than 0.5 m) covers a much larger percentage of area in CPs than in BPs (55.31% compared with 7.71%). Similarly, the upper stratum has greater coverage in CPs (24.63% compared with 14.72% in BPs). In Appendix A, the numerical data of strata distribution of fires can be observed (Table A2).

The coefficient of variation analysis allows us to assess the degree of structural heterogeneity within each stratum (Table 5).

Structural heterogeneity is at its most elevated in the lowest level in all cases, despite having a narrower range (50 cm). Additionally, the differences between burnt sectors and their controls are the greatest in this stratum across all wildfires. There is also a vertical gradient showing decreasing differences in height, even though the range increases with height. The upper stratum shows the least differences, despite having the widest range (in some cases >5 m).

Recent wildfires show statistically significant differences in the lower strata, whereas the 1970 wildfire exhibits significant differences in the lower, intermediate and upper strata. The 1995 wildfire does not show any statistically significant differences.

Table 5. Coefficient of variation by strata, sector and wildfire. Significant differences between burnt sectors and their controls are analyzed by using the Mann–Whitney U test.

	Year 1970		Year 1995		Year 2008		Year 2015	
Metrics	**Burn**	**Control**	**Burnt**	**Control**	**Burnt**	**Control**	**Burnt**	**Control**
<0.5 m	6.846 *	15.999 *	6.112	6.294	21.235 *	6.995 *	11.441 *	15.339 *
0.5 m–1 m	0.156	0.153	0.154	0.140	0.135	0.140	0.136 *	0.147 *
1 m–3 m	0.149 *	0.140 *	0.135	0.105	0.100	0.114	0.098	0.110
3 m–5 m	0.069	0.073	0.069	0.052	0.000	0.051	0.036	0.056
>5 m	0.031 *	0.059 *	0.034	0.075	0.000	0.048	0.000	0.061

* Differences are statistically significant, with a threshold of 0.01.

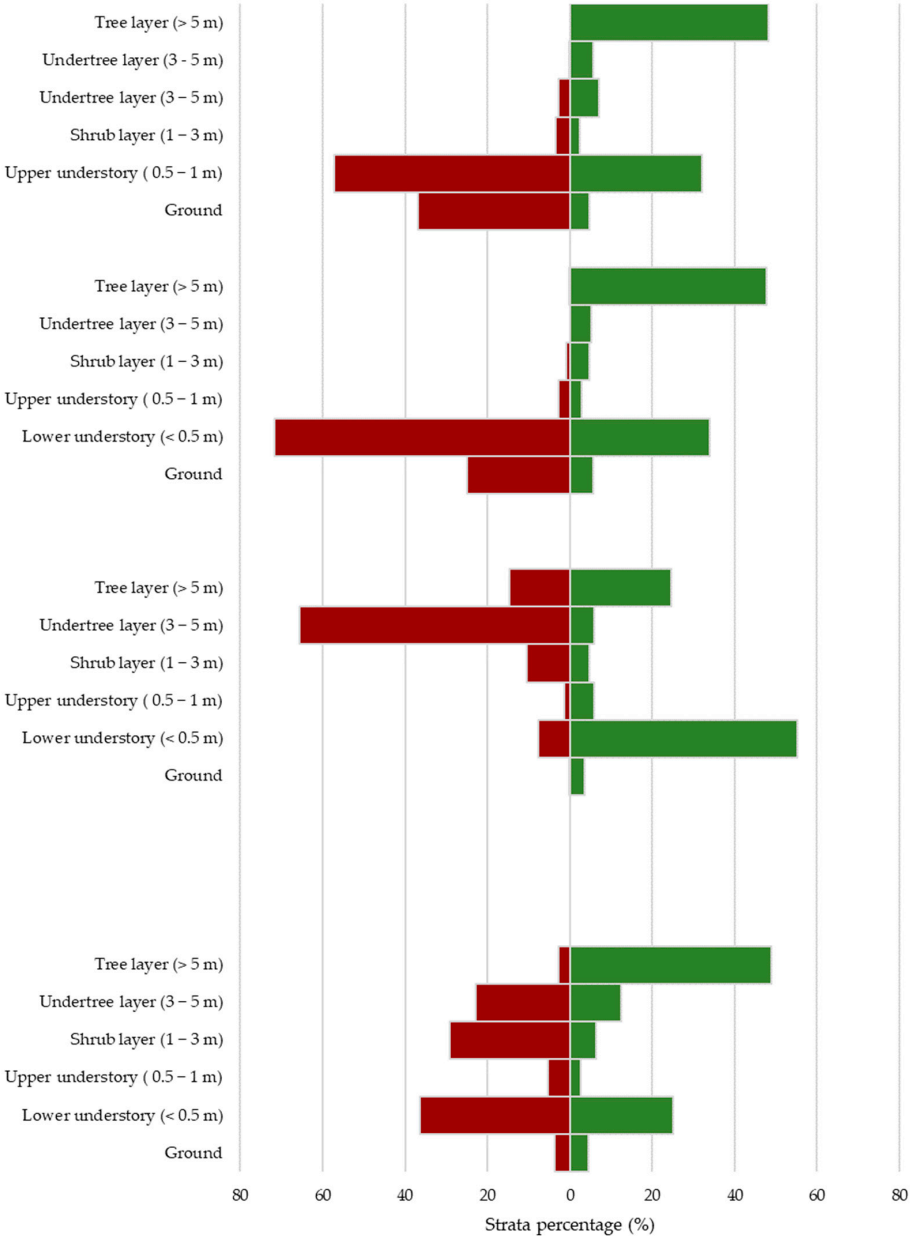

Figure 7. Strata distribution of fires (1970, 1995, 2008 and 2015), arranged chronologically (most recent at the top and oldest at the bottom). Burnt sectors in red and control sectors in green.

4. Discussion

4.1. Methodological Approach

The uni-temporal nature of observations allows for a diachronic analysis of the differences that arise from the impacts that fires have had on forest areas. This is performed by comparing areas unaffected by fires with those that have been affected. This methodological approach, which has been employed in other studies [36,129,130], is supported by: (a) the identification of the Vegetal Community and environmental factors, the contiguity and size of different sectors allowing for this; and (b) the varying chronology of the fires, which enables the analysis of malleability and, consequently, the quantification of ecosystem elasticity.

As we have verified, and as outlined in Section 2.1, severity levels for the different wildfires were obtained from the cartographies by using Montorio et al.'s work (2020), revealing high-severity levels across all analyzed fire areas, consistent with their findings [113]. This approach has also been adopted in other studies for the analysis of Aleppo pine chronosequences [55,131], or through the use of radar data in the same area as our study [129].

However, it is worth noting that this method does not support comparability between the burnt areas or their pre-fire condition, as their respective control areas have undergone their own ecosystem dynamics, potentially resulting in structural and eco-physiological changes. Nevertheless, the post-fire dynamics have been driven by factors that are equally applicable to both burnt and control areas, enabling the methodology to assess the degree of similarity or dissimilarity between them. Therefore, this analysis is considered suitable for use when evaluating malleability and elasticity, both measurable properties that allow for the assessment of resilience in forest ecosystems.

4.2. Physiognomic–Structural Characteristics Related to Resilience

4.2.1. Height Structure and Diversity (Height Mean, 99th Percentile and Coefficient of Variation)

The time factor determines the level of growth—and consequently, recovery—of structures affected by fires [1,82,101,132]. Therefore, one would expect to observe a direct relationship between the degree of growth and post-fire time, leading to a decrease in the magnitude of differences over time between fire-affected areas and analogous unburnt areas.

In the case of **height metrics** (both height mean and P99), a decrease in differences over time, post-disturbance, has been confirmed. However, as noted in the Section 3, the 1995 fire represents a clear anomaly, where height metrics record higher values in the burnt areas. This phenomenon could be explained by the differences in fire intensity, where the temperatures reached during the event were high enough to favor the release of seeds from serotinous cones and the complete combustion—including the destruction of rhizomes—of resprouting species, thereby eliminating competition for the future development of *Pinus halepensis*. As observed, this species can reach greater heights than *Quercus coccifera* and may experience massive and homogeneous growth [133]. Although the geographic proximity between study areas (year–fire) does not suggest differences in structural factors that may explain this phenomenon, a more detailed analysis could be overseen to detect possible situational differences.

Regarding **structural diversity**, there is a detectable increasing pattern related to the age of the fire. The 1970 fire shows greater structural diversity than the more recent fires. Considering that this diversity has a positive ecological effect [134,135], we can determine that older fires, having had more time to stabilize, exhibit a lower degree of malleability and, consequently, greater resilience. The results, however, do not reveal a pattern that explains the variability of differences among the levels analyzed, despite the assumption of low elasticity for these types of formations, where fire is an integral part of their evolutionary dynamics [136]. It would be interesting to know the age of the specimens at the time of the different fires, as the fertility of *P. halepensis* varies over time, ending its juvenile stage at 3–6 years old and reaching reproductive maturity at an age of 15–30 years [137].

4.2.2. Coverage, Relative Shape and Distribution of Strata (Canopy Cover, Canopy Relief Ratio and Strata Percent Coverage)

The **percentage of vegetation cover**, expressed through the Canopy Cover metric, indicates a greater recovery of fire-affected structures over time. Consequently, more similar distributions are observed in the 1970 fire compared with the more recent fires.

Canopy Cover is expected to increase over time [65,101], eventually reaching a point close to its initial state, where the differences between the burnt and control sectors are minimal. Although other studies have reported recovery periods of less than 20 years for these vegetation formations [138,139], it has been observed that this time frame may be insufficient in some cases. This suggests that other factors might be influencing the recovery process, thereby determining the degree of ecosystem elasticity.

In the analyzed fires, the canopy cover was lower in the burnt sectors than in their controls, except for the 1995 fire, which showed an inverse trend, and the 1970 fire, where levels were closer between sectors. Although this study quantifies ecosystem malleability and elasticity, it is plausible that by following the concept of ecological resilience, (see Section 1), alternative stable states could exist. Therefore, it is not necessary that the post-fire situation be identical to the previous one. If actual states are stable enough, they can infer ecosystem resilience [18], in this case, from a structural perspective.

In more recent fires, the canopy cover is very low (almost all cases are found to be below 10% coverage), being even lower in the 2008 fire. Although this fire would be expected to have a greater degree of regeneration than the 2015 fire—given that seven more years have passed—it still presents even lower values.

The 1995 fire stands alone, once again, as an anomaly, showing a massive and homogeneous structure. In this case, the exponential decay models that explain the density evolution of *Pinus halepensis* seedlings [140] do not seem to apply, due to the large number of germinated seedlings. It would be appropriate to analyze whether, as it may seem, the post-fire climatic conditions were ideal for the germination of the dispersed seed bank. However, after four years of monitoring (up to 1999), the regeneration patterns were normal for this species [141]. To reach this level of seedling density, subsequent forestry treatments (mechanized thinning) would need to have been applied in recent years. Although it would be interesting to incorporate this factor into the analysis, there is no systematic record of the information that made this possible.

Regarding the **relative shape of canopy**, which describes the roughness and relative position of the forest canopy, a similar pattern is observed. There is a high degree of similarity between the burnt sector and its control for the 1970 fire, although the control sector shows a pattern that shifts slightly toward the canopy tops compared to the burnt one.

The more recent fires show a high number of pixels with values below 0.5 in BPs and a high number of ground pixels, indicating a significant difference compared to the control sector. Once again, the 1995 fire is an anomaly regarding the expected pattern, as 90% of the pixels register values above 0.5, meaning that canopy surfaces are mostly in the upper portion of the height range, which indicates homogeneous and synchronous germination.

As for the **stratified structure**, as previously mentioned in the more recent fires, we find a clear predominance of bare ground (<0.05 cm) and structures below 0.5 m. This indicates high malleability for these fires, as there are pronounced differences between burnt sectors and their controls.

In the 1995 fire, the undertree level is predominant (>65%), highlighting the homogeneous nature of the structures in the burnt area and a marked difference compared to its control sector. In the case of the 1970 fire, there is a more balanced presence of the different levels in both sectors, although the burnt one has a higher percentage in the upper stratum. This discrepancy can be explained as a long-term effect of the fire, which, as observed in other species of the same genus, leaves its mark for more than 100 years [142].

4.2.3. Canopy Complexity (Profile Area and Profile Area Change)

In terms of canopy complexity, a temporal pattern is once again observed in the magnitude of differences between burnt and control areas. The 1970 fire shows low levels of malleability, as the analysis of PA distribution in the burnt sector is comparable to its control sector, with a PAC value close to zero, although some differences are still detected. The more recent fires exhibit the greatest differences: the LiDAR pulse penetrability is much higher in the burnt areas, because they are much more open, indicating a less complex canopy structure compared to their control sectors. Consequently, these fires show a higher degree of malleability.

There is also a high degree of malleability observed for the 1995 fire, although in this case, the trend is reversed: there is lower penetrability due to the aforementioned process of massive and homogeneous regeneration.

4.3. Search for Potential Explanatory Factors

The methodological approach, based on the collection of LiDAR data, has allowed us to assess the malleability and ecosystem elasticity of *Ph* formations in the Mediterranean environments within the Ebro Basin. Their penetration capacity enables us to characterize the vertically distributed attributes, thus allowing for a more precise analysis of forest canopy structure [143]. The structural dimension is linked to the eco-physiological characteristics of forest systems as it affects understory plant competition, microclimate, recruitment, species diversity and composition [90].

As we have previously touched on, in general terms, a temporal ordering of the magnitude of the differences is observed, regardless of their sign. However, a certain particularity related to the dates of the fires has been detected, so we cannot assume there is high resilience—considering the engineering approach—for these formations in all cases. Although time is one of the main driving factors controlling the recovery process, there may be other factors modulating these processes that underpin resilience within a forest system.

In Mediterranean ecosystems, species exhibit high tolerance thresholds to wildfires, ensuring their continuity despite, and even because of, such events [144–146]. Although **specific species composition** is a determinant of resilience in forest formations, in this case, the predominance of adapted species like *Qc* and *Ph* has minimized the importance of this element as a primary driving factor. This species-specific homogeneity diminishes the explanatory capacity of species composition regarding adaptation mechanisms.

Burn severity determines the state of vegetation at the beginning of the post-fire recovery process. Higher severity has a positive effect on regeneration (lower elasticity) in *Pinus halepensis*, whereas the relationship is reversed for *Quercus coccifera* (higher elasticity) [146]. In the analyzed plots, severity is high for all fires, suggesting it may not be an explanatory factor for interannual differences or for the anomaly observed in the 1995 fire compared to the temporal pattern of differences. Vicente-Serrano et al. (2007) argue that there is no relationship between severity and recovery level for these fires [147]. For the 1970 fire, the severity level could not be evaluated due to a lack of available satellite information.

Hydrological forest treatments also affect the regeneration process as they represent an additional disturbance that can either enhance post-fire degradation or inhibit some of its direct consequences. These treatments alter plant growth processes and have hydrological, erosive and soil consequences that disrupt post-fire ecosystem dynamics. The degree of impact on the ecosystem may depend on the type of treatment applied. A common practice is the removal of burnt wood, which, although it can reduce the risk of pest and disease incidence [148], can result in up to 33% seed mortality and weaken those that survive [149]. Additionally, it is crucial to consider the timing of these treatments, as seedling mortality is higher in smaller-sized plants and during earlier growth stages [150].

In the case of the most recent fires, wood extraction or snag shredding in situ occurred over the first few years following the fire, while for the 1970 fire, we do not have any available information related to this. Although we lack information regarding this issue for

the 1995 fire, it is worthwhile to understand the type of treatment, as well as the phases and timing of the actions, as they may have conditioned or influenced the recovery process.

Climate is a primary conditioning factor as it determines the typology, distribution and dynamics of vegetation across all scales [151,152], and can also be one of the main limiting factors for its development [153]. Insolation and temperature are critical factors influencing biological development and, consequently, forest growth [154]. In the same way, studies indicate that higher levels of humidity lead to burnt surfaces recovering more rapidly [155,156].

Although the climatic conditions are structurally comparable, some studies have described the post-fire natural regeneration of Aleppo pine as irregular, slow and challenging [47,157,158], with the first few years after the fire being critical to the success of the natural recolonization processes. Considering this, the aridification of post-fire climatic conditions may limit natural regeneration [159,160], and consequently may have played a role in explaining the differences found among fires.

In conclusion, post-fire precipitation and temperature levels may explain the regenerative dynamics since these fires. In turn, this makes it necessary to analyze anomalies to determine if thermo-hygrometric conditions have experienced or are experiencing changes compared to normal values, both within and between plots. This factor could emerge as a primary explanatory variable.

In any case, this chronological control of the differences based on the age of the fire, both in terms of malleability—an inverse relationship between time and malleability—and elasticity, indicates that time constitutes a primary control factor. However, the combined action of other factors may be conditioning the degree of resilience within forest ecosystems in Mediterranean areas.

5. Conclusions

The applied methodological approach allows us to analyze the degree of ecosystem malleability and elasticity in forest areas due to the disruption caused by wildfires. Simultaneous data collection ensures homogeneity in terms of data conditions and, together with the spatial connection between burnt areas and control areas, guarantees homogeneous environmental conditions. Nevertheless, analyzing these structural factors is recommended, specifically the morpho-topographic ones, to ensure full comparability between burnt and control areas.

We consider that this methodological approach, along with carrying out an appropriate analysis of structural factors and data collection conditions, can be applied to evaluate the degree of ecosystem resilience in forest areas using remote sensing techniques. This can be performed from a structural perspective (LiDAR data), as well as in terms of composition and functioning, using spectral and/or thermal information.

Malleability decreases over time in forest ecosystems that have been affected by wildfires, which has led to a decreasing temporal order of differences in the analyzed metrics. This applies to height distribution and diversity, as well as to coverage, relative shape, stratification distribution and canopy complexity. Thus, we can confirm that time is the main control factor of these differences and is, therefore, inversely proportional to malleability after a disturbance caused by wildfire. Structurally speaking, elasticity is higher than what has been determined in previous studies.

In any case, a certain particularity has been detected based on the dates of the fires and further substantiated by the anomaly presented by the 1995 fire. Therefore, we can conclude that there are other situational factors that may be influencing the regeneration process and, consequently, affecting ecosystem resilience.

Specific composition, burn severity—homogeneous in our case—or situational climatic conditions (pre- and post-fire) may be modulating the forest regeneration processes. Additionally, the type of post-fire intervention (when applied) can significantly alter the regenerative dynamics and thereby affect resilience. Regardless, it would be interesting to analyze

in future studies how the different types of post-fire treatment (depending on its typology) affect the regenerative processes, at a structural level, in *Pinus halepensis* formations.

Author Contributions: Conceptualization, F.P.-C., S.L.-J. and R.M.; methodology, C.I.C. and S.L.-J.; software, S.L.-J., R.H.M. and C.I.C.; formal analysis, S.L.-J.; research, S.L.-J.; resources, R.H.M. and S.L.-J.; data curation, C.I.C., S.L.-J. and R.H.M.; writing draft preparation, S.L.-J., F.P.-C. and R.M. All authors have read and agreed to the published version of the manuscript.

Funding: This research was funded by MCIN/AEI/10.13039/501100011033, grant number PID2020-118886RB-I00. A predoctoral contract from the 2022–2026 Convocation (Government of Aragon) was awarded to Cristian Iranzo, and, from the Ministry of Universities (FPU18/05027 and FPU FPU22/04489, respectively), contracts were awarded to Raúl Hoffrén and Sergio Larraz-Juan.

Data Availability Statement: The original contributions presented in the study are included in the article, further inquiries can be directed to the corresponding author.

Conflicts of Interest: The authors declare no conflicts of interest.

Appendix A

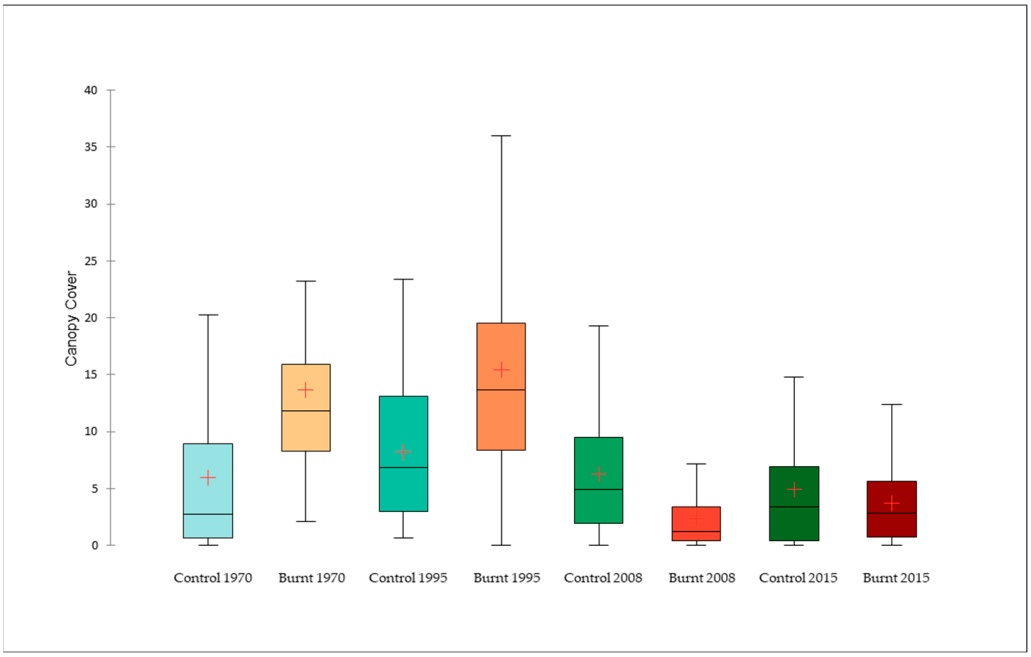

Figure A1. Boxplot of Canopy Cover in different sectors (BP/CP) by year of fire in upper understory strata (0.5 m–1 m). In green, Control Sectors, and in red, Burnt Sectors. Boxes are arranged chronologically (most recent on the left and oldest on the right). The orange cross represents the mean value.

Table A1. Differences between burnt sectors in the analyzed LiDAR metrics by wildfire. Acronyms: CRR = Canopy Relief Ratio; CV = coefficient of variation; Hm = height mean; P99 = 99th percentile; PA = Profile Area. Significant differences between burnt sectors and their controls are analyzed with D-statistic (Kolmogorov-Smirnov test).

	CRR	CV	Hm	P99	PA
1995 vs. 1970	−25.774	52.302	−70.444	−67.747	−61.458
2008 vs. 1970	53.517	−9.169	81.939	83.020	61.670

Table A1. *Cont.*

	CRR	CV	Hm	P99	PA
2015 vs. 1970	57.390	8.005	84.013	85.128	64.868
2008 vs. 1995	78.087	−63.503	97.216	97.319	92.716
2015 vs. 1995	78.159	−46.989	97.447	97.642	92.896
2015 vs. 2008	9.428	21.142	21.549	21.009	8.890

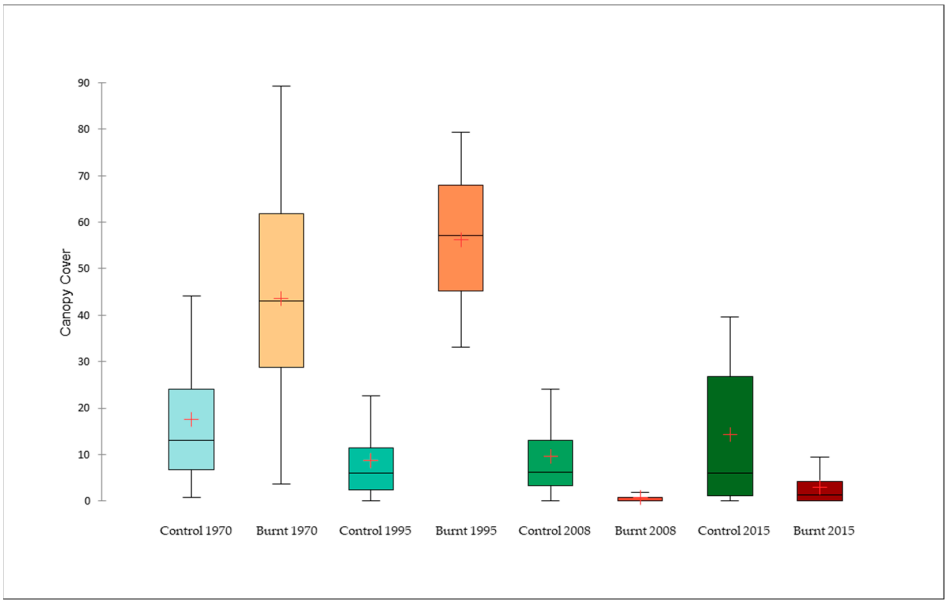

Figure A2. Boxplot of Canopy Cover in different sectors (BP/CP) by year of fire in shrub layer strata (1 m–3 m). In green, Control Sectors, and in red, Burnt Sectors. Boxes are arranged chronologically (most recent on the left and oldest on the right). The orange cross represents the mean value.

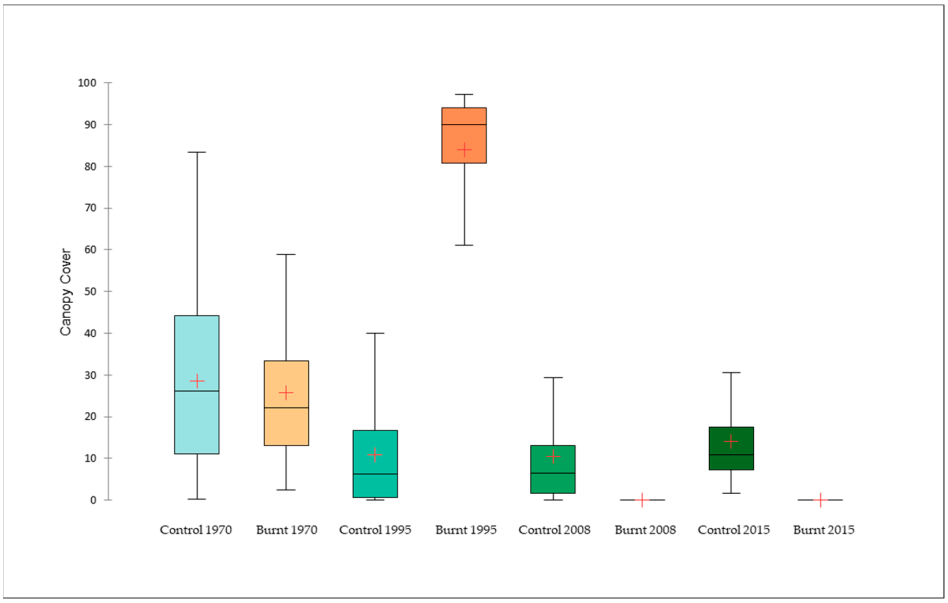

Figure A3. Boxplot of Canopy Cover in different sectors (BP/CP) by year of fire in undertree layer strata (3 m–5 m). In green, Control Sectors, and in red, Burnt Sectors. Boxes are arranged chronologically (most recent on the left and oldest on the right). The orange cross represents the mean value.

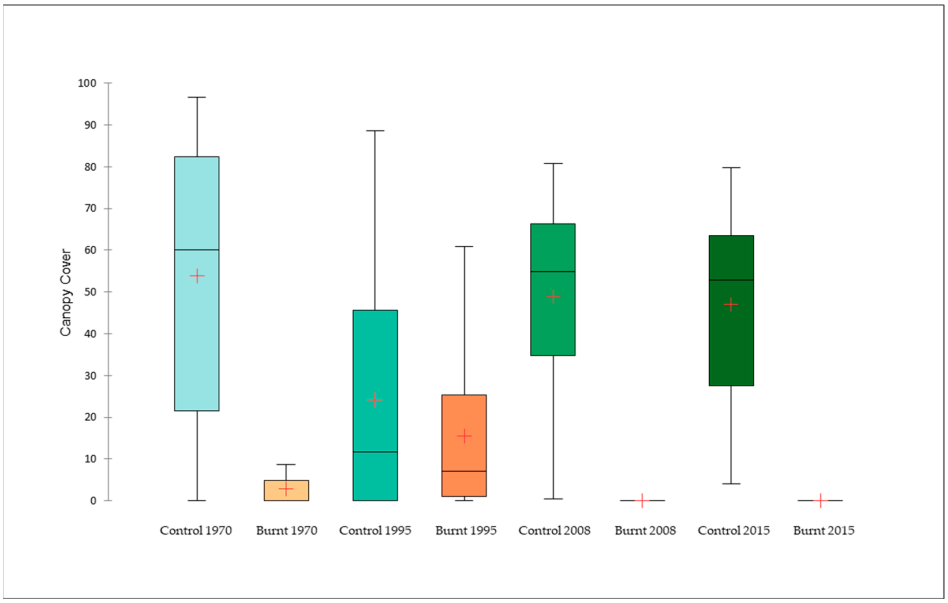

Figure A4. Boxplot of Canopy Cover in different sectors (BP/CP) by year of fire in tree layer strata (upper than 5 m). In green, Control Sectors, and in red, Burnt Sectors. Boxes are arranged chronologically (most recent on the left and oldest on the right). The orange cross represents the mean value.

Table A2. Strata distribution by sector and wildfire.

	Year 1970		Year 1995		Year 2008		Year 2015	
Metrics	**Burn**	**Control**	**Burnt**	**Control**	**Burnt**	**Control**	**Burnt**	**Control**
Ground	3.58	4.56	0.16	3.64	24.88	5.56	36.83	4.81
<0.5 m	36.36	25.09	7.71	55.31	71.64	33.97	57.11	32.05
0.5 m–1 m	5.34	2.67	1.35	5.92	2.71	2.76	3.40	2.35
1 m–3 m	29.09	6.43	10.55	4.68	0.78	4.79	2.65	7.05
3 m–5 m	22.94	12.35	65.52	5.82	0.00	5.12	0.01	5.63
>5 m	2.70	48.9	14.72	24.63	0.00	47.8	0.00	48.11

References

1. González-De Vega, S.; De las Heras, J.; Moya, D. Resilience of Mediterranean terrestrial ecosystems and fire severity in semiarid areas: Responses of Aleppo pine forests in the short, mid and long term. *Sci. Total Environ.* **2016**, *573*, 1171–1177. [CrossRef]
2. Pausas, J.G.; Llovet, J.; Rodrigo, A.; Vallejo, R. Are wildfires a disaster in the Mediterranean basin?—A review. *Int. J. Wildland Fire* **2008**, *17*, 713. [CrossRef]
3. Pausas, J.G.; Vallejo, V.R. The role of fire in European Mediterranean ecosystems. In *Remote Sensing of Large Wildfires*; Chuvieco, E., Ed.; Springer: Berlin/Heidelberg, Germany, 1999; pp. 3–16.
4. Dale, V.H.; Mcnulty, S.G.; Neilson, R.P.; Ayres, M.P.; Flannigan, M.D.; Hanson, P.J.; Irland, L.C.; Lugo, A.E.; Peterson, C.J.; Simberloff, D.; et al. Climate Change and Forest Disturbances. *Bioscience* **2001**, *51*, 723–734. [CrossRef]
5. Dupuy, J.; Fargeon, H.; Martin-StPaul, N.; Pimont, F.; Ruffault, J.; Guijarro, M.; Hernando, C.; Madrigal, J.; Fernandes, P. Climate change impact on future wildfire danger and activity in southern Europe: A review. *Ann. For. Sci.* **2020**, *77*, 35. [CrossRef]
6. IPCC. IPCC Summary for Policymakers. In *Climate Change 2022—Impacts, Adaptation and Vulnerability*; Cambridge University Press: New York, NY, USA, 2023; pp. 3–34.
7. Moritz, M.A.; Parisien, M.-A.; Batllori, E.; Krawchuk, M.A.; Van Dorn, J.; Ganz, D.J.; Hayhoe, K. Climate change and disruptions to global fire activity. *Ecosphere* **2012**, *3*, 1–22. [CrossRef]
8. Pausas, J.G.; Keeley, J.E. Wildfires and global change. *Front. Ecol. Environ.* **2021**, *19*, 387–395. [CrossRef]
9. Bond, W.; Keeley, J. Fire as a Global 'Herbivore': The Ecology and Evolution of Flammable Ecosystems. *Trends Ecol. Evol.* **2005**, *20*, 387–394. [CrossRef]
10. Pausas, J.G.; Keeley, J.E. Evolutionary Fire Ecology: An Historical Account and Future Directions. *Bioscience* **2023**, *73*, 602–608. [CrossRef] [PubMed]

11. Bedia, J.; Herrera, S.; Camia, A.; Moreno, J.M.; Gutiérrez, J.M. Forest fire danger projections in the Mediterranean using ENSEMBLES regional climate change scenarios. *Clim. Change* **2014**, *122*, 185–199. [CrossRef]
12. Handmer, J.; Honda, Y.; Kundzewicz, Z.W.; Arnell, N.; Benito, G.; Hatfield, J.; Mohamed, I.F.; Peduzzi, P.; Wu, S.; Sherstyukov, B.; et al. Changes in Impacts of Climate Extremes: Human Systems and Ecosystems. In *Managing the Risks of Extreme Events and Disasters to Advance Climate Change Adaptation*; Field, C.B., Barros, V., Stocker, T.F., Dahe, Q., Eds.; Cambridge University Press: Cambridge, UK, 2012; pp. 231–290.
13. Mansoor, S.; Farooq, I.; Kachroo, M.M.; Mahmoud, A.E.D.; Fawzy, M.; Popescu, S.M.; Alyemeni, M.N.; Sonne, C.; Rinklebe, J.; Ahmad, P. Elevation in wildfire frequencies with respect to the climate change. *J. Environ. Manag.* **2022**, *301*, 113769. [CrossRef] [PubMed]
14. Nolan, R.H.; Collins, L.; Leigh, A.; Ooi, M.K.J.; Curran, T.J.; Fairman, T.A.; Resco de Dios, V.; Bradstock, R. Limits to post-fire vegetation recovery under climate change. *Plant Cell Environ.* **2021**, *44*, 3471–3489. [CrossRef]
15. Piñol, J.; Terradas, J.; Lloret, F. Climate Warming, Wildfire Hazard, and Wildfire Occurrence in Coastal Eastern Spain. *Clim. Chang.* **1998**, *38*, 345–357. [CrossRef]
16. Turco, M.; Jerez, S.; Augusto, S.; Tarín-Carrasco, P.; Ratola, N.; Jiménez-Guerrero, P.; Trigo, R.M. Climate drivers of the 2017 devastating fires in Portugal. *Sci. Rep.* **2019**, *9*, 13886. [CrossRef] [PubMed]
17. Baho, D.L.; Allen, C.R.; Garmestani, A.; Fried-Petersen, H.; Renes, S.E.; Gunderson, L.; Angeler, D.G. A quantitative framework for assessing ecological resilience. *Ecol. Soc.* **2017**, *22*, art17. [CrossRef]
18. Marcos, B.; Gonçalves, J.; Alcaraz-Segura, D.; Cunha, M.; Honrado, J.P. Assessing the resilience of ecosystem functioning to wildfires using satellite-derived metrics of post-fire trajectories. *Remote Sens. Environ.* **2023**, *286*, 113441. [CrossRef]
19. van Leeuwen, M.; Nieuwenhuis, M. Retrieval of forest structural parameters using LiDAR remote sensing. *Eur. J. For. Res.* **2010**, *129*, 749–770. [CrossRef]
20. García-Ruiz, J.M.; López-Moreno, J.I.; Lasanta, T.; Vicente-Serrano, S.M.; González-Sampériz, P.; Valero-Garcés, B.L.; Sanjuán, Y.; Beguería, S.; Nadal-Romero, E.; Lana-Renault, N.; et al. Los efectos geoecológicos del cambio global en el Pirineo Central español: Una revisión a distintas escalas espaciales y temporales. *Pirineos* **2015**, *170*, e012. [CrossRef]
21. Lloret, F.; Calvo, E.; Pons, X.; Díaz-Delgado, R. Wildfires and landscape patterns in the Eastern Iberian Peninsula. *Landsc. Ecol.* **2002**, *17*, 745–759. [CrossRef]
22. MacDonald, D.; Crabtree, J.R.; Wiesinger, G.; Dax, T.; Stamou, N.; Fleury, P.; Gutierrez Lazpita, J.; Gibon, A. Agricultural abandonment in mountain areas of Europe: Environmental consequences and policy response. *J. Environ. Manag.* **2000**, *59*, 47–69. [CrossRef]
23. Moreira, F.; Viedma, O.; Arianoutsou, M.; Curt, T.; Koutsias, N.; Rigolot, E.; Barbati, A.; Corona, P.; Vaz, P.; Xanthopoulos, G.; et al. Landscape—Wildfire interactions in southern Europe: Implications for landscape management. *J. Environ. Manag.* **2011**, *92*, 2389–2402. [CrossRef]
24. Tattoni, C.; Grilli, G.; Araña, J.; Ciolli, M. The Landscape Change in the Alps—What Postcards Have to Say about Aesthetic Preference. *Sustainability* **2021**, *13*, 7426. [CrossRef]
25. Ursino, N.; Romano, N. Wild forest fire regime following land abandonment in the Mediterranean region. *Geophys. Res. Lett.* **2014**, *41*, 8359–8368. [CrossRef]
26. Díaz-Delgado, R.; Lloret, F.; Pons, X. Influence of fire severity on plant regeneration by means of remote sensing imagery. *Int. J. Remote Sens.* **2003**, *24*, 1751–1763. [CrossRef]
27. Fernández-García, V.; Santamarta, M.; Fernández-Manso, A.; Quintano, C.; Marcos, E.; Calvo, L. Burn severity metrics in fire-prone pine ecosystems along a climatic gradient using Landsat imagery. *Remote Sens. Environ.* **2018**, *206*, 205–217. [CrossRef]
28. Fernandez-Manso, A.; Quintano, C.; Roberts, D.A. Burn severity influence on post-fire vegetation cover resilience from Landsat MESMA fraction images time series in Mediterranean forest ecosystems. *Remote Sens. Environ.* **2016**, *184*, 112–123. [CrossRef]
29. Montorio Llovería, R.; Pérez-Cabello, F.; Vlassova, L.; de la Riva Fernández, J. La severidad del fuego: Revisión de conceptos, métodos y efectos ambientales. In *Geoecología, Cambio Ambiental y Paisaje: Homenaje al Profesor José María García-Ruiz*; Arnáez Vadillo, J., González Sampériz, P., Lasanta Martínez, T., Lorenzo Valero, B., García Ruiz, J.M., Eds.; Consejo Superior de Investigaciones Científicas (CSIC), Instituto Pirenaico de Ecología-Universidad de la Rioja: Logroño, Spain, 2014; pp. 427–440.
30. Vieira, D.C.S.; Fernández, C.; Vega, J.A.; Keizer, J.J. Does soil burn severity affect the post-fire runoff and interrill erosion response? A review based on meta-analysis of field rainfall simulation data. *J. Hydrol.* **2015**, *523*, 452–464. [CrossRef]
31. Bodí, M.B.; Cerdà, A.; Mataix-Solera, J.; Doerr, S.H. Efectos de los incendios forestales en la vegetación y el suelo en la cuenca mediterránea: Revisión bibliográfica. *Bol. Asoc. Geógr. Esp.* **2012**, *58*, 33–55. [CrossRef]
32. Gajendiran, K.; Kandasamy, S.; Narayanan, M. Influences of wildfire on the forest ecosystem and climate change: A comprehensive study. *Environ. Res.* **2024**, *240*, 117537. [CrossRef]
33. Kruger, F.J. Effects of Fire on Vegetation Structure and Dynamics. In *Ecological Effects of Fire in South African Ecosystems*; Booysen, P.V., Tainton, N.M., Eds.; Springer: Berlin/Heidelberg, Germany, 1984; Volume 48, pp. 219–243.
34. Núñez, M.R.; Calvo, L. Effect of High Temperatures on Seed Germination of Pinus Sylvestris and Pinus Halepensis. *For. Ecol. Manag.* **2000**, *131*, 183–190. [CrossRef]
35. Zwolinski, M.J. Fire effects on vegetation and succession. In *Effects of Fire Management of Southwestern Natural Resources*; General Technical Report RM-GTR-191; Krammes, J.S., Ed.; USDA Forest Service: Fort Collins, CO, USA, 1990; Volume RM-GTR-191, pp. 18–24.

36. Pérez-Cabello, F.; Ibarra, P.; Echeverría, M.T.; de la Riva, J. Post-fire Land Degradation of Pinus Sylvestris L. Woodlands after 14 Years. *Land. Degrad. Dev.* **2010**, *21*, 145–160. [CrossRef]
37. Brown, J.K.; Smith, J.K. *Wildland Fire in Ecosystems: Effects of Fire on Flora*; Fort Collins Service Center: For Collins, CO, USA, 2000; Volume RMRS-GTR-42-2.
38. Agbeshie, A.A.; Abugre, S.; Atta-Darkwa, T.; Awuah, R. A review of the effects of forest fire on soil properties. *J. For. Res.* **2022**, *33*, 1419–1441. [CrossRef]
39. Cerdá, A. Changes in overland flow and infiltration after a rangeland fire in a Mediterranean scrubland. *Hydrol. Process* **1998**, *12*, 1031–1042. [CrossRef]
40. Certini, G. Effects of fire on properties of forest soils: A review. *Oecologia* **2005**, *143*, 1–10. [CrossRef]
41. Inbar, A.; Lado, M.; Sternberg, M.; Tenau, H.; Ben-Hur, M. Forest fire effects on soil chemical and physicochemical properties, infiltration, runoff, and erosion in a semiarid Mediterranean region. *Geoderma* **2014**, *221–222*, 131–138. [CrossRef]
42. Pérez-Cabello, F.; Echeverría, M.T.; Ibarra, P.; de la Riva, J. Fire Effects of Fire on Vegetation, Soil and Hydrogeomorphological Behavior in Mediterranean Ecosystems. In *Earth Observation of Wildland Fires in Mediterranean Ecosystems*; Chuvieco, E., Ed.; Springer: Berlin/Heidelberg, Germany, 2009; pp. 154–196.
43. Santín, C.; Doerr, S.H. Fire effects on soils: The human dimension. *Philos. Trans. R. Soc. B Biol. Sci.* **2016**, *371*, 20150171. [CrossRef]
44. Keeley, J.E. Ecology and evolution of pine life histories. *Ann. For. Sci.* **2012**, *69*, 445–453. [CrossRef]
45. Naveh, Z. The evolutionary significance of fire in the mediterranean region. *Vegetatio* **1975**, *29*, 199–208. [CrossRef]
46. Pausas, J.G.; Carbó, E.; Neus Caturla, R.; Gil, J.M.; Vallejo, R. Post-fire regeneration patterns in the eastern Iberian Peninsula. *Acta Oecol.* **1999**, *20*, 499–508. [CrossRef]
47. Trabaud, L.; Michels, C.; Grosman, J. Recovery of burnt *Pinus halepensis* mill. forests. II. Pine reconstruction after wildfire. *For. Ecol. Manag.* **1985**, *13*, 167–179. [CrossRef]
48. Daskalakou, E.; Thanos, C. Aleppo Pine (*Pinus halepensis*) Postfire Regeneration: The Role of Canopy and Soil Seed Banks. *Int. J. Wildland Fire* **1996**, *6*, 59. [CrossRef]
49. Lamont, B.B.; Enright, N.J.; He, T. Fitness and evolution of resprouters in relation to fire. *Plant Ecol.* **2011**, *212*, 1945–1957. [CrossRef]
50. Pausas, J.G. Response of plant functional types to changes in the fire regime in Mediterranean ecosystems: A simulation approach. *J. Veg. Sci.* **1999**, *10*, 717–722. [CrossRef]
51. Schwilk, D.W.; Ackerly, D.D. Flammability and serotiny as strategies: Correlated evolution in pines. *Oikos* **2001**, *94*, 326–336. [CrossRef]
52. Pausas, J.G.; Keeley, J.E. Evolutionary ecology of resprouting and seeding in fire-prone ecosystems. *New Phytol.* **2014**, *204*, 55–65. [CrossRef] [PubMed]
53. Clarke, P.J.; Lawes, M.J.; Midgley, J.J.; Lamont, B.B.; Ojeda, F.; Burrows, G.E.; Enright, N.J.; Knox, K.J.E. Resprouting as a key functional trait: How buds, protection and resources drive persistence after fire. *New Phytol.* **2013**, *197*, 19–35. [CrossRef]
54. Hanes, T.L. Succession after Fire in the Chaparral of Southern California. *Ecol. Monogr.* **1971**, *41*, 27–52. [CrossRef]
55. Kazanis, D.; Spatharis, S.; Kokkoris, G.D.; Dimitrakopoulos, P.G.; Arianoutsou, M. Drivers of *Pinus halepensis* Plant Community Structure across a Post-Fire Chronosequence. *Fire* **2024**, *7*, 331. [CrossRef]
56. Daskalakou, E.N.; Albanis, K.; Skouteri, A.; Thanos, C.A. Predicting Time-Windows for Full Recovery of Postfire Regenerating *Pinus halepensis* Mill. Forests after a Future Wildfire. *New For.* **2014**, *45*, 53–70. [CrossRef]
57. Ne'eman, G.; Arianoutsou, M. Mediterranean Pines—Adaptations to Fire. In *Pines and Their Mixed Forest Ecosystems in the Mediterranean Basin*; Ne'eman, G., Osem, Y., Eds.; Springer: Cham, Switzerland, 2021; Volume 38, pp. 457–480.
58. Daskalakou, E.N.; Thanos, C.A. Postfire Seedling Dynamics and Performance in *Pinus halepensis* Mill. Populations. *Acta Oecol.* **2010**, *36*, 446–453. [CrossRef]
59. Ali, A. Forest stand structure and functioning: Current knowledge and future challenges. *Ecol. Indic.* **2019**, *98*, 665–677. [CrossRef]
60. Jucker, T.; Bongalov, B.; Burslem, D.F.R.P.; Nilus, R.; Dalponte, M.; Lewis, S.L.; Phillips, O.L.; Qie, L.; Coomes, D.A. Topography shapes the structure, composition and function of tropical forest landscapes. *Ecol. Lett.* **2018**, *21*, 989–1000. [CrossRef] [PubMed]
61. Pérez-Cabello, F.; Montorio, R.; Alves, D.B. Remote sensing techniques to assess post-fire vegetation recovery. *Curr. Opin. Environ. Sci. Health* **2021**, *21*, 100251. [CrossRef]
62. Bautista Aguilar, S. Regeneración Post-Incendio de Un Pinar (*Pinus halepensis*, Miller) En Ambiente Semiárido. Erosión Del Suelo y Medidas de Conservación a Corto Plazo. Ph.D. Thesis, Universidad de Alicante, Alicante, Spain, 1999.
63. Moya, D.; González-De Vega, S.; Lozano, E.; García-Orenes, F.; Mataix-Solera, J.; Lucas-Borja, M.E.; de las Heras, J. The Burn Severity and Plant Recovery Relationship Affect the Biological and Chemical Soil Properties of *Pinus halepensis* Mill. Stands in the Short and Mid-Terms after Wildfire. *J. Environ. Manag.* **2019**, *235*, 250–256. [CrossRef] [PubMed]
64. Cerda, A. *Fire Effects on Soils and Restoration Strategies*; Cerdá, A., Robichaud, P., Eds.; CRC Press: Enfield, NH, USA, 2009; ISBN 9781439843338.
65. Gelabert, P.J.; Montealegre, A.L.; Lamelas, M.T.; Domingo, D. Forest structural diversity characterization in Mediterranean landscapes affected by fires using Airborne Laser Scanning data. *GIsci Remote Sens.* **2020**, *57*, 497–509. [CrossRef]
66. Jimeno-Llorente, L.; Marcos, E.; Fernández-Guisuraga, J.M. The Effects of Fire Severity on Vegetation Structural Complexity Assessed Using SAR Data Are Modulated by Plant Community Types in Mediterranean Fire-Prone Ecosystems. *Fire* **2023**, *6*, 450. [CrossRef]

67. Kimmins, J.P. Biodiversity and its relationship to ecosystem health and integrity. *For. Chron.* **1997**, *73*, 229–232. [CrossRef]
68. Holling, C.S. Resilience and Stability of Ecological Systems. *Annu. Rev. Ecol. Syst.* **1973**, *4*, 1–23. [CrossRef]
69. Holling, C.S. *Engineering Within Ecological Constraints*; National Academy of Engineering, Ed.; National Academies Press: Washington, DC, USA, 1996; ISBN 978-0-309-05198-9.
70. Folke, C.; Carpenter, S.R.; Walker, B.; Scheffer, M.; Chapin, T.; Rockström, J. Resilience Thinking: Integrating Resilience, Adaptability and Transformability. *Ecol. Soc.* **2010**, *15*, art20. [CrossRef]
71. Westman, W.E. Measuring the Inertia and Resilience of Ecosystems. *Bioscience* **1978**, *28*, 705–710. [CrossRef]
72. Grimm, V.; Wissel, C. Babel, or the ecological stability discussions: An inventory and analysis of terminology and a guide for avoiding confusion. *Oecologia* **1997**, *109*, 323–334. [CrossRef] [PubMed]
73. Wooster, M.J.; Roberts, G.J.; Giglio, L.; Roy, D.P.; Freeborn, P.H.; Boschetti, L.; Justice, C.; Ichoku, C.; Schroeder, W.; Davies, D.; et al. Satellite remote sensing of active fires: History and current status, applications and future requirements. *Remote Sens. Environ.* **2021**, *267*, 112694. [CrossRef]
74. Bisson, M.; Fornaciai, A.; Coli, A.; Mazzarini, F.; Pareschi, M.T. The Vegetation Resilience After Fire (VRAF) index: Development, implementation and an illustration from central Italy. *Int. J. Appl. Earth Obs. Geoinf.* **2008**, *10*, 312–329. [CrossRef]
75. Chu, T.; Guo, X. Remote Sensing Techniques in Monitoring Post-Fire Effects and Patterns of Forest Recovery in Boreal Forest Regions: A Review. *Remote Sens.* **2013**, *6*, 470–520. [CrossRef]
76. Chuvieco, E.; Mouillot, F.; van der Werf, G.R.; San Miguel, J.; Tanase, M.; Koutsias, N.; García, M.; Yebra, M.; Padilla, M.; Gitas, I.; et al. Historical background and current developments for mapping burned area from satellite Earth observation. *Remote Sens. Environ.* **2019**, *225*, 45–64. [CrossRef]
77. Díaz-Delgado, R.; Lloret, F.; Pons, X.; Terradas, J. Satellite Evidence of Decreasing Resilience in Mediterranean Plant Communities after Recurrent Wildfires. *Ecology* **2002**, *83*, 2293–2303. [CrossRef]
78. Viedma, O.; Meliá, J.; Segarra, D.; Garcia-Haro, J. Modeling rates of ecosystem recovery after fires by using landsat TM data. *Remote Sens. Environ.* **1997**, *61*, 383–398. [CrossRef]
79. Cabello, J.; Paruelo, J.M. La teledetección en estudios ecológicos. *Ecosistemas* **2008**, *17*, 1–3.
80. Fernández-Guisuraga, J.M.; Suárez-Seoane, S.; Calvo, L. Radiative transfer modeling to measure fire impact and forest engineering resilience at short-term. *ISPRS J. Photogramm. Remote Sens.* **2021**, *176*, 30–41. [CrossRef]
81. Frazier, A.E.; Renschler, C.S.; Miles, S.B. Evaluating post-disaster ecosystem resilience using MODIS GPP data. *Int. J. Appl. Earth Obs. Geoinf.* **2013**, *21*, 43–52. [CrossRef]
82. Risna, R.A.; Prasetyo, L.B.; Lughadha, E.N.; Aidi, M.N.; Buchori, D.; Latifah, D. Forest resilience research using remote sensing and GIS—A systematic literature review. *IOP Conf. Ser. Earth Environ. Sci.* **2023**, *1266*, 012086. [CrossRef]
83. Szpakowski, D.; Jensen, J. A Review of the Applications of Remote Sensing in Fire Ecology. *Remote Sens.* **2019**, *11*, 2638. [CrossRef]
84. Jucker, T.; Gosper, C.R.; Wiehl, G.; Yeoh, P.B.; Raisbeck-Brown, N.; Fischer, F.J.; Graham, J.; Langley, H.; Newchurch, W.; O'Donnell, A.J.; et al. Using multi-platform LiDAR to guide the conservation of the world's largest temperate woodland. *Remote Sens. Environ.* **2023**, *296*, 113745. [CrossRef]
85. Magnussen, S.; Wulder, M.A. Post-Fire Canopy Post-Fire Canopy Height Recovery in Canada's Boreal Forests Using Airborne Laser Scanner (ALS). *Remote Sens.* **2012**, *4*, 1600–1616. [CrossRef]
86. McCarley, T.R.; Kolden, C.A.; Vaillant, N.M.; Hudak, A.T.; Smith, A.M.S.; Wing, B.M.; Kellogg, B.S.; Kreitler, J. Multi-temporal LiDAR and Landsat quantification of fire-induced changes to forest structure. *Remote Sens. Environ.* **2017**, *191*, 419–432. [CrossRef]
87. Viana-Soto, A.; García, M.; Aguado, I.; Salas, J. Assessing post-fire forest structure recovery by combining LiDAR data and Landsat time series in Mediterranean pine forests. *Int. J. Appl. Earth Obs. Geoinf.* **2022**, *108*, 102754. [CrossRef]
88. Bergen, K.M.; Goetz, S.J.; Dubayah, R.O.; Henebry, G.M.; Hunsaker, C.T.; Imhoff, M.L.; Nelson, R.F.; Parker, G.G.; Radeloff, V.C. Remote sensing of vegetation 3-D structure for biodiversity and habitat: Review and implications for lidar and radar spaceborne missions. *J. Geophys. Res. Biogeosci* **2009**, *114*. [CrossRef]
89. Coops, N.C.; Hilker, T.; Wulder, M.A.; St-Onge, B.; Newnham, G.; Siggins, A.; Trofymow, J.A. Estimating canopy structure of Douglas-fir forest stands from discrete-return LiDAR. *Trees* **2007**, *21*, 295. [CrossRef]
90. Jarron, L.R.; Coops, N.C.; MacKenzie, W.H.; Tompalski, P.; Dykstra, P. Detection of sub-canopy forest structure using airborne LiDAR. *Remote Sens. Environ.* **2020**, *244*, 111770. [CrossRef]
91. Mandl, L.; Stritih, A.; Seidl, R.; Ginzler, C.; Senf, C. Spaceborne LiDAR for characterizing forest structure across scales in the European Alps. *Remote Sens. Ecol. Conserv.* **2023**, *9*, 599–614. [CrossRef]
92. Atkins, J.W.; Bohrer, G.; Fahey, R.T.; Hardiman, B.S.; Morin, T.H.; Stovall, A.E.L.; Zimmerman, N.; Gough, C.M. Quantifying vegetation and canopy structural complexity from terrestrial LiDAR data using the FORESTR R package. *Methods Ecol. Evol.* **2018**, *9*, 2057–2066. [CrossRef]
93. Atkins, J.W.; Costanza, J.; Dahlin, K.M.; Dannenberg, M.P.; Elmore, A.J.; Fitzpatrick, M.C.; Hakkenberg, C.R.; Hardiman, B.S.; Kamoske, A.; LaRue, E.A.; et al. Scale dependency of lidar-derived forest structural diversity. *Methods Ecol. Evol.* **2023**, *14*, 708–723. [CrossRef]
94. Karna, Y.K.; Penman, T.D.; Aponte, C.; Hinko-Najera, N.; Bennett, L.T. Persistent changes in the horizontal and vertical canopy structure of fire-tolerant forests after severe fire as quantified using multi-temporal airborne lidar data. *For. Ecol. Manag.* **2020**, *472*, 118255. [CrossRef]

95. Alonzo, M.; Morton, D.C.; Cook, B.D.; Andersen, H.-E.; Babcock, C.; Pattison, R. Patterns of canopy and surface layer consumption in a boreal forest fire from repeat airborne lidar. *Environ. Res. Lett.* **2017**, *12*, 065004. [CrossRef]
96. García, M.; North, P.; Viana-Soto, A.; Stavros, N.E.; Rosette, J.; Martín, M.P.; Franquesa, M.; González-Cascón, R.; Riaño, D.; Becerra, J.; et al. Evaluating the potential of LiDAR data for fire damage assessment: A radiative transfer model approach. *Remote Sens. Environ.* **2020**, *247*, 111893. [CrossRef]
97. Hoe, M.S.; Dunn, C.J.; Temesgen, H. Multitemporal LiDAR improves estimates of fire severity in forested landscapes. *Int. J. Wildland Fire* **2018**, *27*, 581. [CrossRef]
98. Kane, V.R.; North, M.P.; Lutz, J.A.; Churchill, D.J.; Roberts, S.L.; Smith, D.F.; McGaughey, R.J.; Kane, J.T.; Brooks, M.L. Assessing fire effects on forest spatial structure using a fusion of Landsat and airborne LiDAR data in Yosemite National Park. *Remote Sens. Environ.* **2014**, *151*, 89–101. [CrossRef]
99. Montealegre, A.; Lamelas, M.; Tanase, M.; De la Riva, J. Forest Fire Severity Assessment Using ALS Data in a Mediterranean Environment. *Remote Sens.* **2014**, *6*, 4240–4265. [CrossRef]
100. Ross, C.W.; Loudermilk, E.L.; O'Brien, J.J.; Flanagan, S.A.; McDaniel, J.; Aubrey, D.P.; Lowe, T.; Hiers, J.K.; Skowronski, N.S. Lidar-derived estimates of forest structure in response to fire frequency. *Fire Ecol.* **2024**, *20*, 44. [CrossRef]
101. Dainelli, R.; Toscano, P.; Di Gennaro, S.F.; Matese, A. Recent Advances in Unmanned Aerial Vehicle Forest Remote Sensing—A Systematic Review. Part I: A General Framework. *Forests* **2021**, *12*, 327. [CrossRef]
102. Dainelli, R.; Toscano, P.; Di Gennaro, S.F.; Matese, A. Recent Advances in Unmanned Aerial Vehicles Forest Remote Sensing—A Systematic Review. Part II: Research Applications. *Forests* **2021**, *12*, 397. [CrossRef]
103. Guimarães, N.; Pádua, L.; Marques, P.; Silva, N.; Peres, E.; Sousa, J.J. Forestry Remote Sensing from Unmanned Aerial Vehicles: A Review Focusing on the Data, Processing and Potentialities. *Remote Sens.* **2020**, *12*, 1046. [CrossRef]
104. Domingo, D.; Lamelas, M.T.; García, M.B. Characterization of vegetation structural changes using multi-temporal LiDAR and its relationship with severity in Calcena wildfire. *Ecosistemas* **2021**, *30*, 1–10. [CrossRef]
105. Hoffrén, R.; Lamelas, M.T.; de la Riva, J. UAV-derived photogrammetric point clouds and multispectral indices for fuel estimation in Mediterranean forests. *Remote Sens. Appl.* **2023**, *31*, 100997. [CrossRef]
106. Wallace, L.; Musk, R.; Lucieer, A. An Assessment of the Repeatability of Automatic Forest Inventory Metrics Derived From UAV-Borne Laser Scanning Data. *IEEE Trans. Geosci. Remote Sens.* **2014**, *52*, 7160–7169. [CrossRef]
107. Carvajal-Ramírez, F.; Marques da Silva, J.R.; Agüera-Vega, F.; Martínez-Carricondo, P.; Serrano, J.; Moral, F.J. Evaluation of Fire Severity Indices Based on Pre- and Post-Fire Multispectral Imagery Sensed from UAV. *Remote Sens.* **2019**, *11*, 993. [CrossRef]
108. Hillman, S.; Hally, B.; Wallace, L.; Turner, D.; Lucieer, A.; Reinke, K.; Jones, S. High-Resolution Estimates of Fire Severity—An Evaluation of UAS Image and LiDAR Mapping Approaches on a Sedgeland Forest Boundary in Tasmania, Australia. *Fire* **2021**, *4*, 14. [CrossRef]
109. Qi, Y.; Coops, N.C.; Daniels, L.D.; Butson, C.R. Assessing the effects of burn severity on post-fire tree structures using the fused drone and mobile laser scanning point clouds. *Front. Environ. Sci.* **2022**, *10*, 949442. [CrossRef]
110. Pérez-Rodríguez, L.A.; Quintano, M.d.C.; García-Llamas, P.; Fernández-García, V.; Taboada, A.; Fernández-Guisuraga, J.M.; Marcos, E.; Suarez-Seoane, S.; Calvo, L.; Fernández-Manso, A. Using Unmanned Aerial Vehicles (UAV) for forest damage monitoring in south-western Europe. In Proceedings of the Imaging Spectrometry XXIII: Applications, Sensors, and Processing, San Diego, CA, USA, 11–15 August 2019; Ientilucci, E.J., Ed.; SPIE: Bellingham, WA, USA; Volume 11130.
111. Pineda Valles, H.E.; Nunes, G.M.; Berlinck, C.N.; Gonçalves, L.G.; Ribeiro, G.H.P.d.M. Use of Remotely Piloted Aircraft System Multispectral Data to Evaluate the Effects of Prescribed Burnings on Three Macro-habitats of Pantanal, Brazil. *Remote Sens.* **2023**, *15*, 2934. [CrossRef]
112. Samiappan, S.; Hathcock, L.; Turnage, G.; McCraine, C.; Pitchford, J.; Moorhead, R. Remote Sensing of Wildfire Using a Small Unmanned Aerial System: Post-Fire Mapping, Vegetation Recovery and Damage Analysis in Grand Bay, Mississippi/Alabama, USA. *Drones* **2019**, *3*, 43. [CrossRef]
113. Montorio, R.; Pérez-Cabello, F.; Borini Alves, D.; García-Martín, A. Unitemporal approach to fire severity mapping using multispectral synthetic databases and Random Forests. *Remote Sens. Environ.* **2020**, *249*, 112025. [CrossRef]
114. Tobler, W. On the First Law of Geography: A Reply. *Ann. Assoc. Am. Geogr.* **2004**, *94*, 304–310. [CrossRef]
115. Cacho Nerín, C.; Sendra Ferrer, J.; Sanz Arauz, G.; Buisán Sanz, S.; Cantón Tobajas, S.; Julve del Val, J.; Miralles Francés, F.; Cortés Rabinad, F.; Lafragüeta Pérez, C. Análisis meteorológico y del comportamiento del fuego del gran incendio forestal de Zuera (Zaragoza) de 5 de agosto de 2008. In Proceedings of the 5° Congreso Forestal Español, Montes y Sociedad: Saber qué Hacer, Ávila, Spain, 21–25 September 2009.
116. Cuadrat, J.M.; Saz, M.A.; Vicente-Serrano, S.M. *Atlas Climático de Aragón*; Gobierno de Aragón: Aragón, Spain, 2007.
117. Montealegre, A.L.; Lamelas, M.T.; De La Riva, J.; García-Martín, A.; Escribano, F. Use of low point density ALS data to estimate stand-level structural variables in Mediterranean Aleppo pine forest. *Forestry* **2016**, *89*, 373–382. [CrossRef]
118. Evans, J.S.; Hudak, A.T. A multiscale curvature algorithm for classifying discrete return LiDAR in forested environments. *IEEE Trans. Geosci. Remote Sens.* **2007**, *45*, 1029–1038. [CrossRef]
119. Montealegre, A.L.; Lamelas, M.T.; Tanase, M.A.; De la Riva, J. Estimación de la severidad en incendios forestales a partir de datos LiDAR-PNOA y valores de Composite Burn Index. *Rev. Teledetección* **2017**, *49*, 1. [CrossRef]
120. Torresan, C.; Corona, P.; Scrinzi, G.; Valls Marsal, J. Using classification trees to predict forest structure types from LiDAR data. *Ann. For. Res.* **2016**, *59*, 281–298. [CrossRef]

121. Korhonen, L.; Korhonen, K.; Rautiainen, M.; Stenberg, P. Estimation of forest canopy cover: A comparison of field measurement techniques. *Silva Fenn.* **2006**, *40*, 577–588. [CrossRef]
122. Atkins, J.W.; Fahey, R.T.; Hardiman, B.S.; Gough, C.M. Forest Canopy Structural Complexity and Light Absorption Relationships at the Subcontinental Scale. *J. Geophys. Res. Biogeosci.* **2018**, *123*, 1387–1405. [CrossRef]
123. Gough, C.M.; Atkins, J.W.; Fahey, R.T.; Hardiman, B.S. High Rates of Primary Production in Structurally Complex Forests. *Ecology* **2019**, *100*, e02864. [CrossRef] [PubMed]
124. Valladares, F.; Laanisto, L.; Niinemets, Ü.; Zavala, M.A. Shedding Light on Shade: Ecological Perspectives of Understorey Plant Life. *Plant Ecol. Divers.* **2016**, *9*, 237–251. [CrossRef]
125. Hakkenberg, C.R.; Zhu, K.; Peet, R.K.; Song, C. Mapping Multi-scale Vascular Plant Richness in a Forest Landscape with Integrated Li <scp>DAR</Scp> and Hyperspectral Remote-sensing. *Ecology* **2018**, *99*, 474–487. [CrossRef]
126. Hu, T.; Ma, Q.; Su, Y.; Battles, J.J.; Collins, B.M.; Stephens, S.L.; Kelly, M.; Guo, Q. A simple and integrated approach for fire severity assessment using bi-temporal airborne LiDAR data. *Int. J. Appl. Earth Obs. Geoinf.* **2019**, *78*, 25–38. [CrossRef]
127. Bertrand, G. Pour Une Étude Géographique de La Végétation. *Rev. Geogr. Pyren. Sud. Ouest* **1966**, *37*, 129–144. [CrossRef]
128. Sheskin, D.J. *Handbook of Parametric and Nonparametric Statistical Procedures*; Chapman and Hall/CRC: Boca Raton, FL, USA, 2003; ISBN 9780429186165.
129. Tanase, M.; de la Riva, J.; Santoro, M.; Pérez-Cabello, F.; Kasischke, E. Sensitivity of SAR data to post-fire forest regrowth in Mediterranean and boreal forests. *Remote Sens. Environ.* **2011**, *115*, 2075–2085. [CrossRef]
130. Vlassova, L.; Pérez-Cabello, F. Effects of post-fire wood management strategies on vegetation recovery and land surface temperature (LST) estimated from Landsat images. *Int. J. Appl. Earth Obs. Geoinf.* **2016**, *44*, 171–183. [CrossRef]
131. Kaye, J.P.; Romanyà, J.; Vallejo, V.R. Plant and Soil Carbon Accumulation Following Fire in Mediterranean Woodlands in Spain. *Oecologia* **2010**, *164*, 533–543. [CrossRef] [PubMed]
132. Rodrigues, M.; de la Riva, J.; Domingo, D.; Lamelas, T.; Ibarra, P.; Hoffrén, R.; García-Martín, A. An empirical assessment of the potential of post-fire recovery of tree-forest communities in Mediterranean environments. *For. Ecol. Manag.* **2024**, *552*, 121587. [CrossRef]
133. Daskalakou, E.N.; Thanos, C.A. Postfire regeneration of Aleppo pine—The temporal pattern of seedling recruitment. *Plant Ecol. (Former. Veg.)* **2004**, *171*, 81–89. [CrossRef]
134. Ishii, H.T.; Tanabe, S.; Hiura, T. Exploring the Relationships Among Canopy Structure, Stand Productivity, and Biodiversity of Temperate Forest Ecosystems. *For. Sci.* **2004**, *50*, 342–355. [CrossRef]
135. LaRue, E.A.; Hardiman, B.S.; Elliott, J.M.; Fei, S. Structural diversity as a predictor of ecosystem function. *Environ. Res. Lett.* **2019**, *14*, 114011. [CrossRef]
136. Keeley, J.E.; Pausas, J.G. Evolutionary Ecology of Fire. *Annu. Rev. Ecol. Evol. Syst.* **2022**, *53*, 203–225. [CrossRef]
137. Thanos, C.A.; Daskalakou, E.N. Reproduction in *Pinus halepensis* and *P. brutia*. In *Ecology, Biogeography and Management of Pinus halepensis and P. brutia Forest Ecosystems in the Mediterranean Basin*; Neèman, G., Trabaud, L., Eds.; Backhuys Publishers: Leiden, The Netherlands, 2000; pp. 79–90.
138. Màrcia, E.; Iraima, V.; Francisco, L.; Josep Maria, E. Recruitment and growth decline in *Pinus halepensis* populations after recurrent wildfires in Catalonia (NE Iberian Peninsula). *For. Ecol. Manag.* **2006**, *231*, 47–54. [CrossRef]
139. Rodrigues, M.; Ibarra, P.; Echeverría, M.; Pérez-Cabello, F.; de la Riva, J. A method for regional-scale assessment of vegetation recovery time after high-severity wildfires. *Prog. Phys. Geogr. Earth Environ.* **2014**, *38*, 556–575. [CrossRef]
140. Hett, J.M.; Loucks, O.L. Age Structure Models of Balsam Fir and Eastern Hemlock. *J. Ecol.* **1976**, *64*, 1029–1044. [CrossRef]
141. Pérez Grijalbo, J.P.; Pérez Grijalbo, R. Evolución de La Vegetación Tras El Incendio de Los Pinares de Zuera de 1995. *Nat. Aragonesa* **2001**, *7*, 58–69.
142. Adámek, M.; Hadincová, V.; Wild, J. Long-term effect of wildfires on temperate Pinus sylvestris forests: Vegetation dynamics and ecosystem resilience. *For. Ecol. Manag.* **2016**, *380*, 285–295. [CrossRef]
143. Wulder, M.A.; White, J.C.; Nelson, R.F.; Næsset, E.; Ørka, H.O.; Coops, N.C.; Hilker, T.; Bater, C.W.; Gobakken, T. Lidar sampling for large-area forest characterization: A review. *Remote Sens. Environ.* **2012**, *121*, 196–209. [CrossRef]
144. Forner, A.; Valladares, F.; Bonal, D.; Granier, A.; Grossiord, C.; Aranda, I. Extreme droughts affecting Mediterranean tree species' growth and water-use efficiency: The importance of timing. *Tree Physiol.* **2018**, *38*, 1127–1137. [CrossRef] [PubMed]
145. Moya, D.; Espelta, J.M.; Verkaik, I.; López-Serrano, F.; De Las Heras, J. Tree density and site quality influence on *Pinus halepensis* Mill. reproductive characteristics after large fires. *Ann. For. Sci.* **2007**, *64*, 649–656. [CrossRef]
146. Pausas, J.G.; Ribeiro, E.; Vallejo, R. Post-fire regeneration variability of *Pinus halepensis* in the eastern Iberian Peninsula. *For. Ecol. Manag.* **2004**, *203*, 251–259. [CrossRef]
147. Vicente-Serrano, S.M.; Pérez-Cabello, F.; Lasanta, T. *Pinus halepensis* regeneration after a wildfire in a semiarid environment: Assessment using multitemporal Landsat images. *Int. J. Wildland Fire* **2011**, *20*, 195. [CrossRef]
148. Castro, J.; Leverkus, A.; Marañón-Jiménez, S.; Serrano-Ortiz, P.; Sánchez-Cañete, E.P.; Reverter, B.R.; Guzmán-Álvarez, J.R.; Kowalski, A.S. Efecto del manejo de la madera quemada sobre la restauración y regeneración post-incendio: Implicaciones para la gestión y para el conjunto del ecosistema. In Proceedings of the 6° Congreso Forestal Español, Vitoria-Gasteiz, Spain, 10–14 June 2013; Montes Servicios y Desarrollo Rural. Sociedad Española de Ciencias Forestales: Vitoria-Gasteiz, Spain, 2013.
149. Martínez-Sánchez, J.J.; Ferrandis, P.; de las Heras, J.; María Herranz, J. Effect of burnt wood removal on the natural regeneration of *Pinus halepensis* after fire in a pine forest in Tus valley (SE Spain). *For. Ecol. Manag.* **1999**, *123*, 1–10. [CrossRef]

150. Girona-García, A.; Vieira, D.C.S.; Silva, J.; Fernández, C.; Robichaud, P.R.; Keizer, J.J. Effectiveness of post-fire soil erosion mitigation treatments: A systematic review and meta-analysis. *Earth Sci. Rev.* **2021**, *217*, 103611. [CrossRef]
151. Mather, J.R.; Yoshioka, G.A. The Role of Climate in the Distribution of Vegetation. *Ann. Assoc. Am. Geogr.* **1968**, *58*, 29–41. [CrossRef]
152. Roerink, G.J.; Menenti, M.; Soepboer, W.; Su, Z. Assessment of climate impact on vegetation dynamics by using remote sensing. *Phys. Chem. Earth Parts A/B/C* **2003**, *28*, 103–109. [CrossRef]
153. Horion, S.; Cornet, Y.; Erpicum, M.; Tychon, B. Studying interactions between climate variability and vegetation dynamic using a phenology based approach. *Int. J. Appl. Earth Obs. Geoinf.* **2013**, *20*, 20–32. [CrossRef]
154. van der Maarel, E. Vegetation dynamics: Patterns in time and space. *Vegetatio* **1988**, *77*, 7–19. [CrossRef]
155. Elvira, N.J.; Lloret, F.; Jaime, L.; Margalef-Marrase, J.; Pérez Navarro, M.Á.; Batllori, E. Species climatic niche explains post-fire regeneration of Aleppo pine (*Pinus halepensis* Mill.) under compounded effects of fire and drought in east Spain. *Sci. Total Environ.* **2021**, *798*, 149308. [CrossRef] [PubMed]
156. Mendez-Cartin, A.L.; Coll, L.; Valor, T.; Torné-Solà, G.; Ameztegui, A. Post-fire growth of *Pinus halepensis*: Shifts in the mode of competition along a precipitation gradient. *For. Ecol. Manag.* **2024**, *554*, 121693. [CrossRef]
157. Herranz, J.M.; de las Heras, J.; Martínez Sánchez, J.J. Efecto de la orientación sobre la recuperación de la vegetación natural tras el fuego en el valle del río Tus (Yeste, Albacete). *Ecología* **1991**, *5*, 111–124.
158. Trabaud, L. Survie de Jeunes Plantules de Pin d'alep Apparues Apres Incende. *Stud. Oecol.* **1988**, *5*, 161–170.
159. Cabanillas Saldaña, A.M. Bases para la Gestión de Masas Naturales de *Pinus halepensis* Mill. en el Valle del Ebro. Ph.D. Thesis, Universidad Politécnica de Madrid (E.T.S.I. Montes), Madrid, Spain, 2010.
160. Herranz Sanz, J.M. Aspectos botánicos y ecológicos del pino carrasco (*Pinus halepensis* Mill.). *Cuad. Soc. Esp. Cienc. For.* **2000**, *10*, 13–17.